5-14-2010

Numerical and Experimental Analysis of a TurboPiston Pump

Jason A. Kent
University of New Orleans

Numerical and Experimental Analysis of a TurboPiston Pump

A Thesis

Submitted to the Graduate Faculty of the
University of New Orleans
in partial fulfillment of the
requirements for the degree of

Master of Science
in
Mechanical Engineering

by

Jason Allen Kent

B.S. University of New Orleans, 2008

May, 2010

Acknowledgement

I would like to take this opportunity to thank my advisor, Dr. Ting Wang, for his guidance and support while working under him as both an undergraduate and postgraduate student. Without Dr. Ting Wang's hard work and dedication to his students and the University of New Orleans, none of this would be made possible. I would also like to thank, Dr. Kazim Akyuzlu, Dr. Martin Guillot, and Dr. Carsie Hall for being a part of my thesis committee. Furthermore, I would like to thank my fellow colleague students and researchers, Armin Silaen, Lei Zhao, Liang Wang, and others from the Energy Conversion and Conservation Center (ECCC) for their help and support.

I would like to thank Mr. Patrick Rousset of Power Engineering Inc. for providing this project to work on, along with Mr. Robert Brown of JRB Pattern Inc. for manufacturing the TurboPiston Pump. Further, I would like to thank Louisiana Board of Regents Industrial Ties Research Subprogram and Clean Power and Energy Research Consortium (CPERC) for helping fund this project.

Finally, I would like to thank all my family and friends for their support throughout the years while I pursed both, my Bachelors of Science and Masters of Science degree in Mechanical Engineering. They have always been there for me with constant support in dealing with difficult times and made the good times even more enjoyable, and for that I am very grateful.

Table of Contents

List of Figures

List of Tables

Nomenclature

a	local speed of sound (m/s)
c	concentration (mass/volume, moles/volume)
c_p	heat capacity at constant pressure (J/kg-K)
c_v	heat capacity at constant volume (J/kg-K)
D	mass diffusion coefficient (m^2/s)
D_H	hydraulic diameter (m)
D_{ij}	mass diffusion coefficient (m^2/s)
D_t	turbulent diffusivity (m^2/s)
E	total energy (J)
F	force (N)
g	gravitational acceleration (m/s^2)
Gr	Grashof number ($L^3.\rho^2.g.\beta.\Delta T/\mu^2$)
H	total enthalpy (W/m^2-K)
h	species enthalpy (W/m^2-K)
h	height (m)
J	mass flux; diffusion flux (kg/m^2-s)
k	turbulence kinetic energy (m^2/s^2)
k	thermal conductivity (W/m-K)
m	mass (kg)
M_W	molecular weight (kg/kgmol)
M	Mach number
p	pressure (atm)
Pr	Prandtl number (ν/α)
q	heat flux
q_r	radiation heat flux
R	universal gas constant
S	source term
Sc	Schmidt number (ν/D)
t	time (s)
T	temperature (K)
U	mean velocity (m/s)
X	mole fraction (dimensionless)
Y	mass fraction (dimensionless)
x, y, z	coordinates

Greek letter

β	coefficient of thermal expansion (K^{-1})
ε	turbulence dissipation (m^2/s^3)
ε_w	wall emissivity
κ	von Karman constant
μ	dynamics viscosity (kg/m-s)
μ_k	turbulent viscosity (kg/m-s)
ν	kinematic viscosity (m^2/s)

ρ density (kg/m^3)
ρ_w wall reflectivity
σ Stefan-Boltzmann constant
σ_s scattering coefficient
τ stress tensor (kg/m-s^2)

Abstract

The TurboPiston Pump was invented to make use of merits such as, high flow rates often seen in centrifugal pumps and high pressures associated with positive displacement pumps. The objective of this study is to manufacture a plastic model 12" TurboPiston Pump to demonstrate the working principle and a metal prototype for performance testing. In addition, this research includes the study of the discharge valve to estimate the valve closing time and fluid mass being recycled back into the cylinder through hand calculations. Furthermore, a transient simulation was performed in CFD using Fluent to provide a better estimate of what will happen in the actual pump while running. Additionally, an experimental rig was designed to investigate the performance of the first generation valve on the TurboPiston Pump known as the flapper valve. Means to improve the hydrodynamic performance of both valves have been identified for future study.

Keywords: TurboPiston Pump, Centrifugal Pump, Piston Pump, Valve, CFD, Dynamic Mesh, Fluent, Ansys

Chapter One

Introduction

The ability to move water and other fluids from one location to another has been an essential need for mankind since the earliest of times. Before the invention of the pump, this was usually done by means of gravity feed canals for purposes of irrigation and city water distribution. However, with the advent of the pump, plumbing systems were developed to integrate water delivery systems throughout households and large buildings.

Pumps are used in all industries in every corner of the Earth. Two of the most widely used types of pumps are the centrifugal and the positive displacement types. Each pump has its advantages and disadvantages. The centrifugal pump is capable of moving very large quantities of a fluid, but it is only able to impose a relatively low differential pressure to the working fluid. To obtain high pressures, centrifugal pumps are typically setup in series with one another (multistage) to raise the pressure of the working fluid in stages. The downside to this is that multiple pumps are required which drastically decrease the efficiency and increases the weight, and cost, and the amount of space required to obtain the desired flow rate and pressure. The positive displacement pump, on the other hand, is capable of producing very high differential pressures, but in order to obtain a high flow rate, the pump must be enormous in size or several pumps are needed to work in parallel with one another. In either case, the cost is significantly driven up.

A new type of pump has come onto the scene that blends the characteristics of both the positive displacement pump and the centrifugal pump. This is the TurboPiston pump (TPP) which was invented by Mr. Patrick Roussett. The TPP's capability of moving high volumes of fluid at high pressures in one stage makes the TurboPiston pump very efficient and versatile in applications, and is ideal for use in city drainage networks, large oil pipelines, deep-sea drilling, high-rise fire extinguishing, and precision high flow rate pumping.

1.1 Types of Pumps

The function of a pump is to move fluids by increasing the energy of the fluid. This energy, often in the form of kinetic energy can than also be converted into other forms of energy such as pressure by adding resistance to the flow. Pumps have multiple applications such as

agriculture, manufacturing, oil and gas industry, and food processing industry. Depending on the application, a different type of pump may be used to achieve the requirements. Of the many different types of pumps available as seen in Fig. 1.11, two main classification categories can be formed, i.e. Positive Displacement and Dynamic Pumps.

1.1.1 Positive Displacement Pumps

Positive displacement pumps work by displacing a volume of fluid by mechanical means. By knowing the volume displacement, precise amounts of fluids may be pumped for any given application. Furthermore, this allows for a constant flow rate even if upstream conditions change. Positive displacement pumps are often known for being able to produce high outlet pressures. The discharge pressure from the pump is only dependent on power input to the pump and the structural strength of the pump components. Additionally, they also have the advantage of being able to pump viscous fluids easily compared to Dynamic pumps. However, these pumps often require a inlet charge pump to keep the suction pressure above the vapor pressure of the fluid being pumped to help reduce chances of cavitation. Positive displacement pumps can be divided into two sub-categories based off their mechanical motion:

- Rotary
- Reciprocating

Rotary pumps are given their respective name based off the motion of the components. As the rotor turns for each revolution, a volume is created that fills with fluid and is displaced at the outlet. A few rotary pumps are shown and discussed in more detail:

- Sliding vane
- Flexible impeller
- Screw
- Gear
- Lobe
- Axial piston pump

Sliding vane pumps work by allowing vanes to slide in and out of slots in an eccentric rotor. As the eccentric rotor turns, the vanes follow the contour of a cylinder which they slide against. The eccentricity between the rotor and cylinder wall create a volume which displaces

the fluid from inlet to outlet. A diagram of a vane pump can be seen in Fig. 1.1 to help better visualize the internal workings of it.

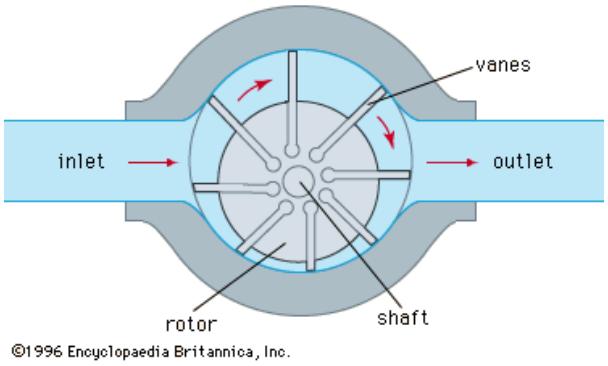

Figure 1.1 Vane Pump

A flexible impeller pump as seen in Fig 1.2 resembles that of a vane pump, however instead of having a rotor that is eccentric to a cylinder, the rotor is concentric and the cylinder does not form a complete circle. It works by having a flexible paddle wheel shaped rotor that rotates along the cylinder walls. As the flexible paddles turn against the bulge in the cylinder wall the volume created between the paddles decreases causing the fluid to be discharged. Due to the flexible nature of the rotor, these pumps are not able to pump at high pressures and are more suited towards thinner fluids rather than viscous fluids. Another variation of this pump also seen in Fig 1.2 is a flexible tube that forms a half arc. A cam then turns against the flexible tube forcing the fluid within out at the discharge.

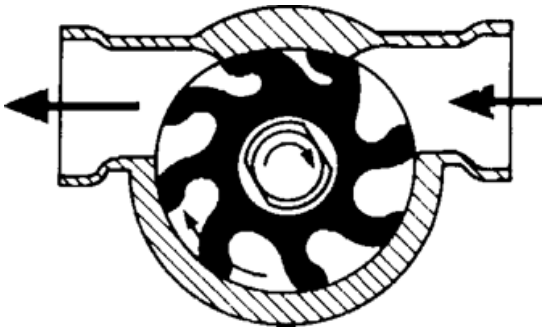

Figure 1.2 Flexible Impeller Pump

Screw pumps as seen in Fig 1.3 are positive displacement pumps through which the fluid is transported between the screw threads on an axis. These pumps consist of a single screw or multiple screws where the threads mesh together forming a seal. Screw pumps are capable of

handling very high pressures and can operate at high speed. The screw pump offers low mechanical vibration, pulsation free flow and quiet operation.

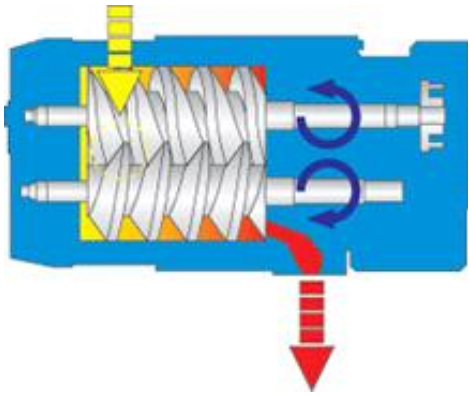

Figure 1.3 Screw Pump

Gear pumps work by incorporating two or more gears that are meshed together. The gears form a seal between the outer edge of the teeth and cylindrical shaped housing. The clearance between the walls must be small to reduce flow leakage. As the gears rotate, the fluid fills the space between the gear teeth and travels along the cylinder from the inlet to the outlet where it is discharged. Fig 1.4 shows a gear pump configuration.

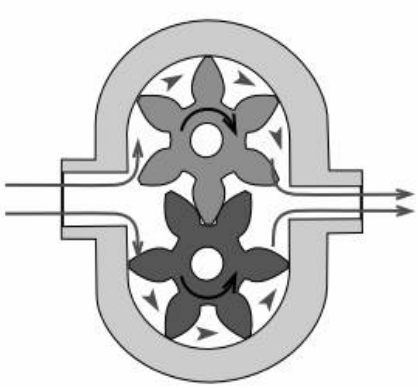

Figure 1.4 Gear Pump

The lobe pump as seen in Fig 1.5 is very similar in concept to that of the gear pump in that two lobes rotate and allow fluid to travel on the outer boundary between the lobes and the casing. One of the major differences is that one lobe is not driven directly by the other. Instead, the lobes are driven by timing gears. Lobe pumps are usually able to handle larger volumes of fluid per revolution compared to that of the gear pump and are able to permit larger particle in the fluid due to the increased volume size created between the lobes and casing.

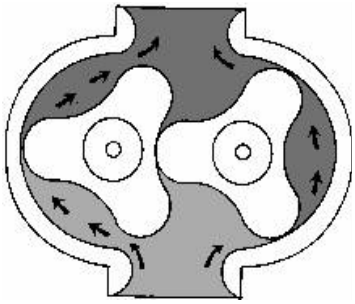

Figure 1.5 Lobe Pump

In axial piston pumps, Fig. 1.6, the cylinders and the drive shaft are parallel. The reciprocating motion is created by a cam plate, also known as a swash plate, tilting plate, or wobble plate. This plate is stationary and lies in a plane that cuts across the centerline of the drive shaft and cylinder barrel. In a fixed-displacement pump, the cam plate is set at an angle of approximately 25 degrees from the perpendicular plane of the pump centerline. Variable-delivery axial piston pumps are designed so the angle the cam plate makes will be perpendicular to the centerline of the cylinder barrel and may vary from zero to approximately 25 degrees to one or both sides. One end of each piston rod is held in contact with the cam plate. When the cylinder block rotates, the piston assembly rotates with it. Meanwhile, the pistons follow the angled swash plate, thus causing the pistons to move in and out of the cylinder block as the pump rotates. The length of the piston stroke is proportional to the angle that the cam plate is set from the perpendicular line to the centerline of the cylinder barrel.

Other variations of this pump include the bent axis piston pump as seen in Fig 1.7. The bent axis piston pump eliminates the swash plate by having the cylinder block set at an angle to that of the drive shaft. To vary the pump displacement, the cylinder block and valve plate are mounted in a yoke, and the entire assembly is swung in an arc around a pair of mounting pins attached to the pump housing.

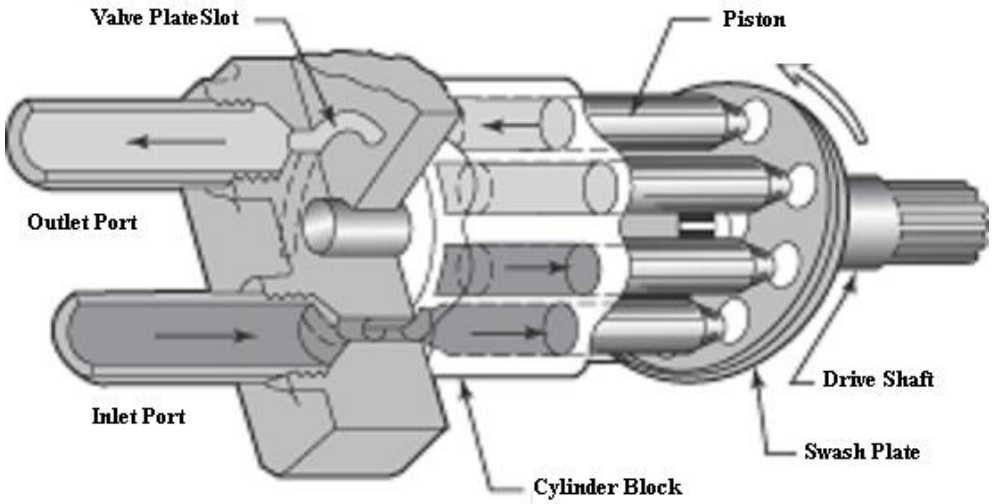

Figure 1.6 Axial Piston Pump

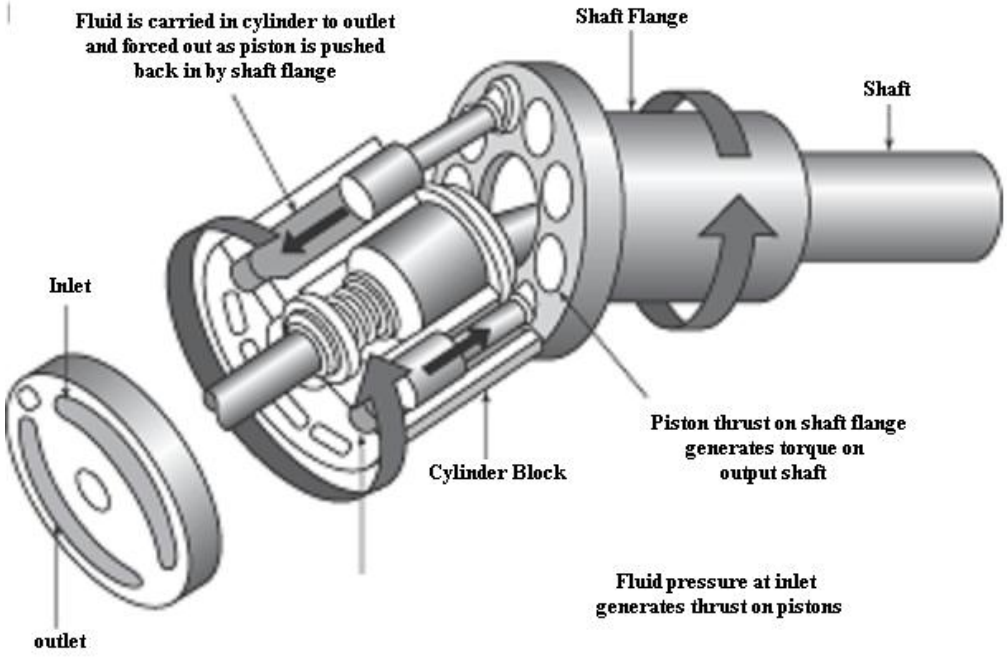

Figure 1.7 Bent Axis Piston Pump

Both the axial piston pump and bent axis piston pump cylinders are filled with the pumping fluid as they rotate. The fluid enters a valve plate which has arc slots which allows fluid to flow through. As the pistons go through the expansion stroke, they draw fluid into the cylinder through the valve plate. Similarly, when the pump is discharging, fluid is forced through another circular arc on the valve plate and then to the discharge port.

1.1.2 Dynamic Pumps

Dynamic pumps generate pressure by transferring energy to the fluid by using either centrifugal force, reaction force from blades or a combination of both. The way in which energy is transferred is used to classify dynamic pumps as follows:

- Radial flow
- Axial flow
- Mixed flow

In general, dynamic pumps provide a higher flow rate than positive displacement pumps and a much steadier discharge but are ineffective in handling high-viscosity liquids. Dynamic pumps also generally need priming i.e., they cannot suck a fluid from a reservoir into the inlet. The positive displacement pump on the other hand, is self-priming for almost any application. However, most positive displacement pumps require a charge pump upstream to help reduce chances of cavitation.

In radial pumps such as a centrifugal pump shown in Fig. 1.8, the fluid enters at the eye of the impeller. From here, the impeller blades rotates the fluid, thus imparting kinetic energy to the fluid and accelerating it outwards in the radial direction. Once the fluid exits the impeller, the fluid usually goes through a diffuser where the high velocity is converted into pressure head. Centrifugal pumps are capable of high flow rates; however the pressure is usually small unless multiple stages are used.

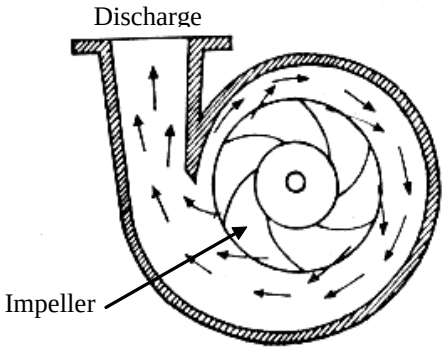

Figure 1.8 Centrifugal Pump

In an axial flow pump shown in Fig. 1.9, the impeller pushes the liquid in a direction parallel to the pump shaft. Axial flow pumps are sometimes called propeller pumps. These

pumps develop most of their pressure by imparting energy into the fluid through design of blade geometry.

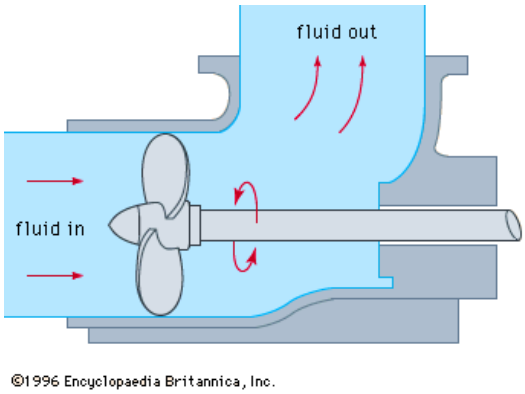

Figure 1.9 Axial Flow Pump

A mixed flow pump as seen in Fig 1.10 is a pump in which the head is developed partly by centrifugal force and partly by the lift of the vanes on the liquid. This type of pump has a single inlet impeller with the flow entering axially and discharging in an axial/radial direction.

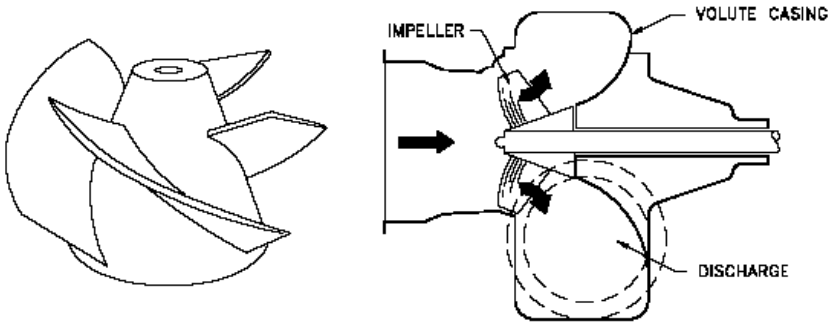

Figure 1.10 Mixed Flow Impeller

As seen, it is evident that many different types of pumps exist. The selection of a pump depends on many variables set by the requirements of different applications. Figure 1.11 summarizes all the different types of pumps from dynamic to positive displacement pumps by breaking them down into categories.

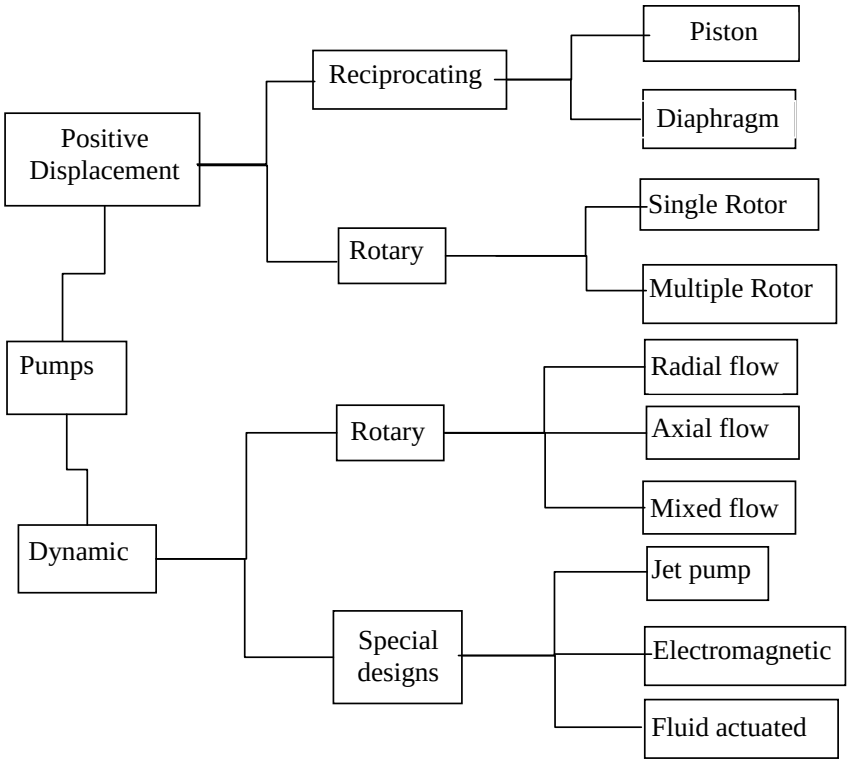

Figure 1.11 Classification of Pumps

1.2 TurboPiston Pump

The TurboPiston Pump (TPP) is a revolutionary new pump containing the features of both dynamic and positive displacement pumps. It was invented to take advantage of the merits of the two different pump classifications while discarding the disadvantages of each. The pump is capable of obtaining high pressures often seen in positive displacement pumps while also obtaining high flow rates often seen in dynamic pumps. Furthermore, the TurboPiston Pump has a very small footprint to that of pumps with similar pressures and flow rate.

Any new product that is introduced to the market will not survive unless there is a demand for the product. In the case of the TPP, many industries have a need for the pump in applications that require multiple pumps or multiple stages to accomplish the same task that the TPP can achieve in a single stage. A comparison of the TPP specifications compared to that of other common pumps can be seen in Fig. 1.12-1.14.

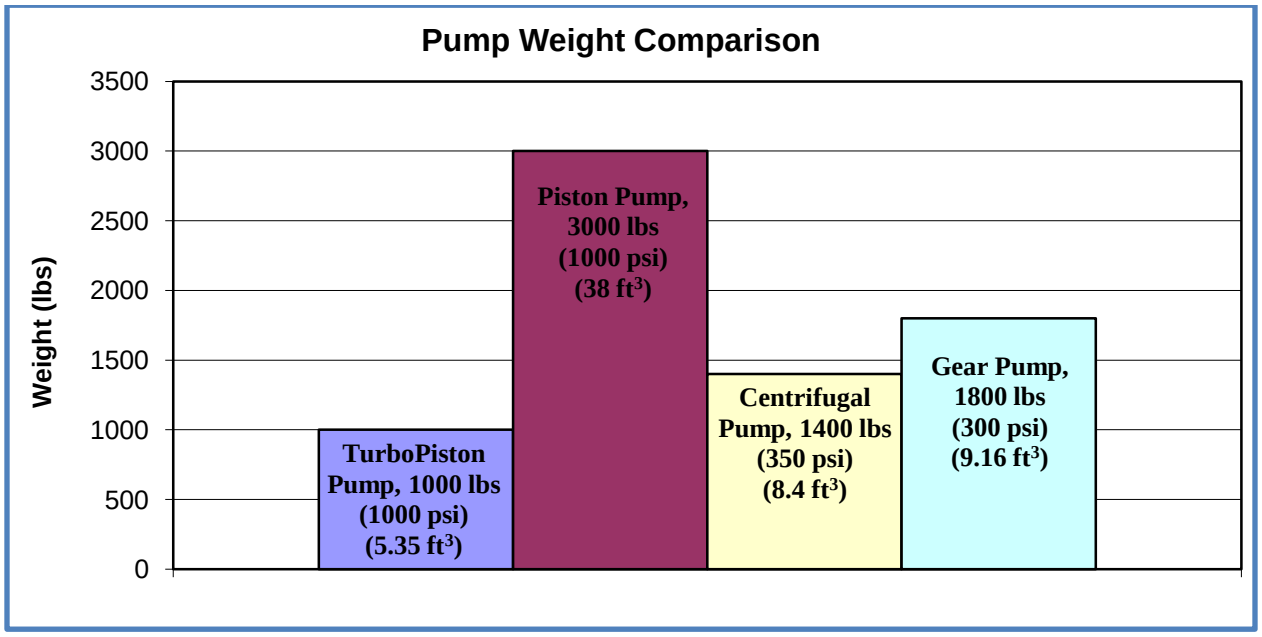

Figure 1.12 TPP Weight Comparison with similar flow rates of approximately 650 GPM. No single-stage centrifugal or gear pump is available for comparison at 1000 psi.

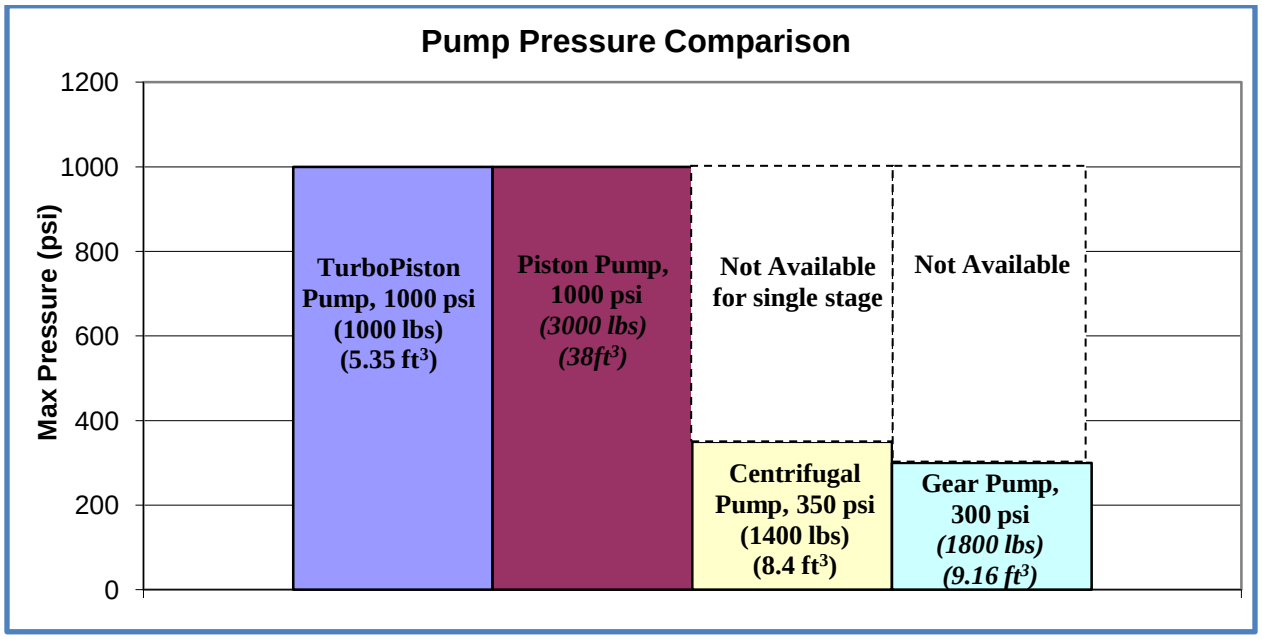

Figure 1.13 TPP Pressure Comparison with similar flow rates of approximately 650 GPM.

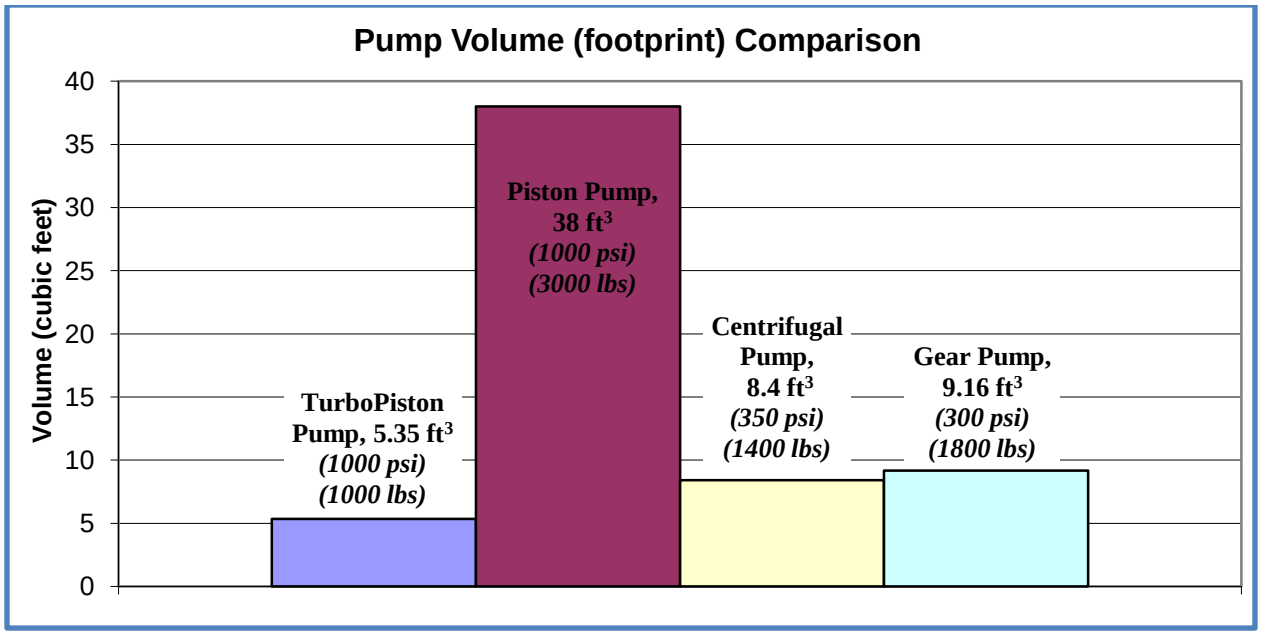

Figure 1.14 TPP Volumetric Footprint Comparison with similar flow rates of approximately 650 gpm.

The pump works by sucking fluid into the intake as seen in Fig 1.15 at location [1] where it flows through a centrifugal impellor. The impellor boosts the head pressure [2] via centrifugal force before entering into the valves of the cylinder assembly [3]. This effectively allows the fluid to flow at higher rates while decreasing the chances of cavitation through the small valve passages. The fluid is then drawn into the piston cylinders [4] on the suction stroke and positively displaced at the outlet at high pressure [5].

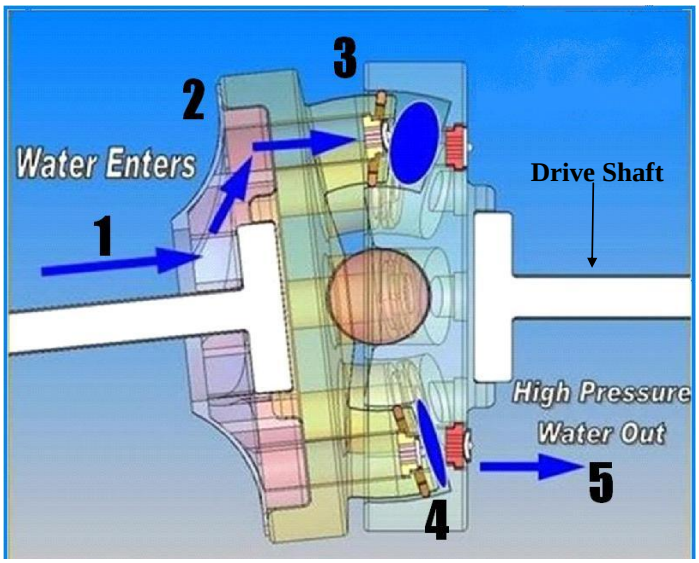

Figure 1.15 TPP Water Flow Passage

1.3 Pump Performance

The performance of a pump can be determined using a pump performance curve as shown in Fig 1.16. The performance curve is a plot of head pressure vs. flow rate and is developed for a specific pump through testing. Usually development of a pump performance curve starts by closing off the valve at the discharge end completely. This will give you a maximum head pressure when the flow rate is zero. This is often known as the shutoff head. The valve is then slowly opened allowing fluid to flow through and the flow rate and head pressure is plotted multiple times on the chart until the flow rate reaches a maximum and the head pressure reaches a minimum.

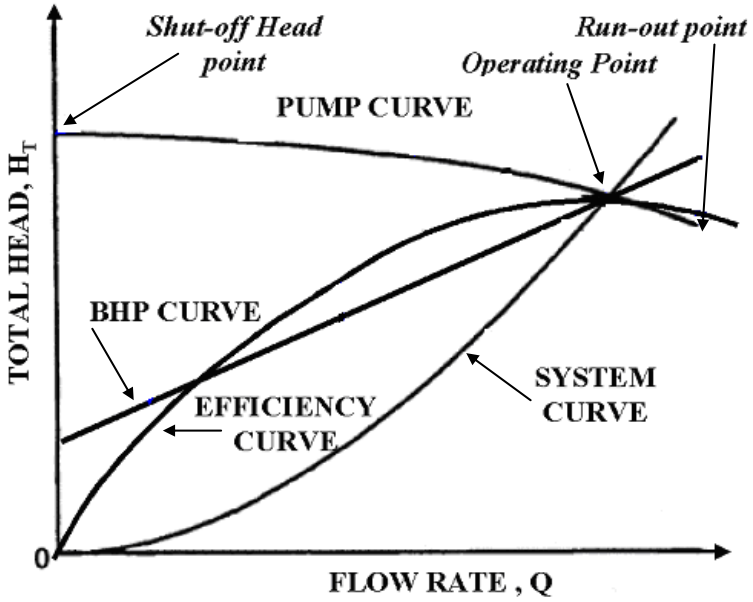

Figure 1.16 Pump Performance Curve

Furthermore, often seen on the pump performance curve is the efficiency curve and power curve. This shows the pumps efficiency through its full range of flow rates and the power required to achieve the given performance. The efficiency of a pump is defined by the power transmitted to the fluid divided by the shaft power of the pump as seen below. The power transmitted to the fluid can be defined by the product of the flow rate, head pressure and specific gravity of the fluid being pumped.

$$\eta_p = \frac{\text{power gained by fluid}}{\text{pump shaft power}} = \frac{P_f}{\dot{W}_{shaft}}$$

1.4 Objectives

The TurboPiston Pump has potential to revolutionize the pump industry by giving customers an affordable pump capable of handling both high pressure and high flow rates. However, the pump is currently only in the testing phase and a lot of developmental problems have to be worked out before the pump can be put on the market. A demonstration model is the first step in bringing the pump from an idea to reality. The demonstration model gives investors a tangible object to see and invest money into. A test model can then be developed and heavily tested to find potential problems from which improvements can be made. Areas of improvement range from improving piston seal leakage and life to improving the inlet and discharge valves. Valves are a source of resistance, turbulent eddies, and cavitation which are suspected to be a major contributor to pump efficiency. The objective of this study is to conduct research, aid in the design, and testing of the TurboPiston Pump to help bring it to market. The specific goals are:

1. Produce a hand-cranking 12" acrylic demonstration model to show the pump working principle.
2. Produce a working 12" metal pump for testing and certification
3. Identify several potential or current issues with the TurboPiston Pump and come up with possible solutions
4. Use computational fluid dynamics (CFD) to calculate the flow field and better understand both the flow behavior and valve movement inside the TPP
5. Build a valve visualization flow experimental test rig to help better understand the flow structure around the TPP valves to improve pump efficiency.

Chapter Two

Design and Fabrication of TurboPiston Pump Demonstration and Test Models

The TurboPiston Pump came about through the pursuit of pushing the performance limit of pumps currently available on the market by incorporating three major pump parameters often not seen together and combining them into a single pump. Specifically, increasing head pressure to that of most conventional positive displacement pumps, increasing flow rate to that of most centrifugal pumps, while at the same time reducing the overall pump footprint.

Taking on this challenge proved to be difficult, not only because a whole new pump was being developed, but also because no other pump like it has been created with the same features that are incorporated into the TurboPiston Pump. Consequently, no baseline or standards were available to use as a starting point. Therefore, after the initial design was finished, demonstration models were needed for proof of concept and for testing and certification of the innovative design.

2.1 Initial Design

The TurboPiston Pump design came about by incorporating the high flow rates of centrifugal pumps, high pressure of positive displacement pumps and trying to keep the size down to a minimum in a single pump. With this envision in mind, a pump was designed using current pump technologies.

2.1.1 Major Components

Centrifugal Impeller

Starting at the pump inlet, the fluid first flows to the centrifugal impeller. The impeller increases head pressure as the fluid travels in the radial direction outwards towards the cylinder intake port. This effective increase in head pressure allows for higher velocities through the valves by increasing the fluids total pressure, thus allowing higher flow rates through the pump while reducing the possibility of cavitation. The impeller also serves as the inlet guide to allow flow to moves smoothly towards each cylinder intake port. Figure 2.1 shows the TPP cast impeller.

Figure 2.1 TurboPiston Pump cast centrifugal impeller

Piston Assembly

Positive displacement pumps are able to obtain high pressure; however, it's often not feasible to obtain high flow rates through only one or three cylinders as in the design of most piston type positive displacement pumps. Thus, a similar design of many hydraulic pumps, namely the axial piston pump and bent axis piston pump with multiple pistons were chosen. Furthermore, this reduces the complexity of the pump by eliminating the often complex crank geometry used to achieve the piston reciprocating motion by mounting eight pistons on a single disk that rotates. The eight corresponding cylinders are then mounted on a separate disk with an offset angle. The angle created between the two rotating disks creates a wedge of volume. As the two disks rotate in unison, the pistons move in and out of the cylinder positively displacing water at a high pressure. Figure 2.2 shows both the TPP piston rotor and cylinder rotor.

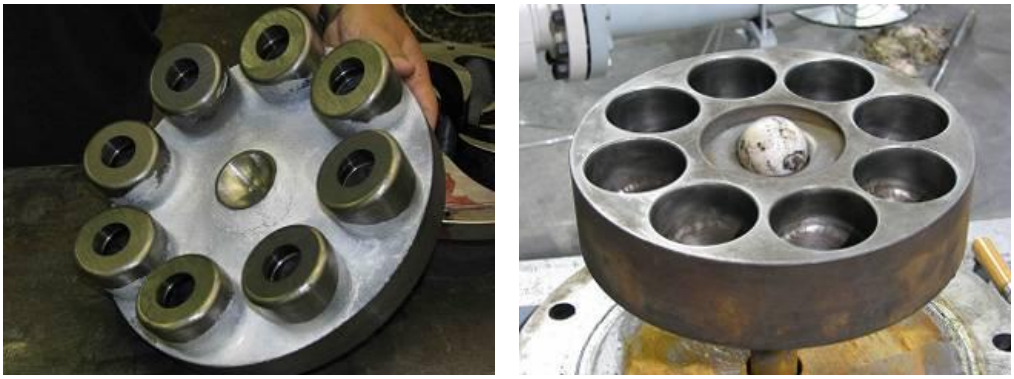

Figure 2.2 TurboPiston Pump piston and cylinder rotor

2.1.2 Sub-Components

Valves

The valves on the TurboPiston Pump started out as a "flapper valve" design. This valve design works like a check valve in which fluid is only allowed to flow in one direction. The flapper valve design was chosen because of its simplicity and fast response. The flapper valve for both the intake and discharge are the same and consist of a main valve body which has flow passages machined into it. A rubber disk located on one side of the valve body covers the flow passages. As fluid flows through the valve, the rubber disk folds back allowing fluid to pass. The flapper shuts and seals against the valve body when it is under adverse pressure gradient, thus preventing flow from traveling backwards.

With the flapper valve design continuously having problems, another type of valve called the piston valve was designed as a second option to continue on with the pump development. This valve consists of a valve and stem, which slides in and out of a valve body. The discharge valve opens when fluid is forced out the cylinder into the discharge region of the pump and closes due to the pressure differential across the valve. Figure 2.3 shows both the flapper valve and piston valve used on the TPP.

Flapper Valve Piston Valve

Figure 2.3 TurboPiston Pump flapper and piston valve assemblies

Bearings

The bearings on the TurboPiston Pump are located near the intake and discharge section of the TurboPiston Pump. Figure 2.4 show the locations of the inlet and discharge bearings on the TPP. The bearings are required to take both axial and radial loads due to the pump design. For instance, the pump cylinder rotor is cantilevered into the pump casing. Due to the large

weight of the rotor and the cantilever distance, large radial loads are present. Furthermore, the pressure differential across the cylinder and discharge region creates an axial thrust load that must be counteracted by the bearings. Caged roller bearings were selected for both the inlet and discharge section due to their ability to take both axial and radial loads.

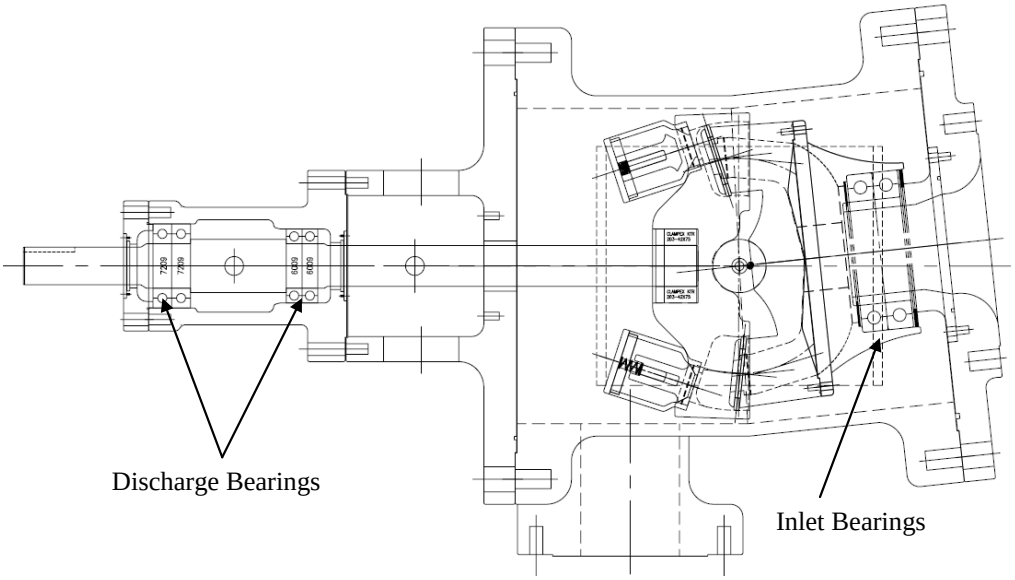

Figure 2.4 Bearing locations on TurboPiston Pump (Top view)

The bearings on the TurboPiston Pump at the inlet and centrifugal impeller have to be sealed. This is because one side of the bearing is exposed to the high discharge pressure pump fluid while the other side of the bearing is exposed to the lower intake pressure. If not properly sealed, fluid will flow through the bearings causing the pump to leak and possibly cause the bearings to fail with a loss of bearing lubrication as the water flows through.

2.2 Acrylic TurboPiston Pump Concept Model

The acrylic TurboPiston Pump shown in Fig. 2.5 was developed as a demonstration model to show proof of concept and help clearly show the interior design and the working principal of TPP. The acrylic model was made by JPB Innovation in Greeenville, South Carolina. The manufacturing process is described below.

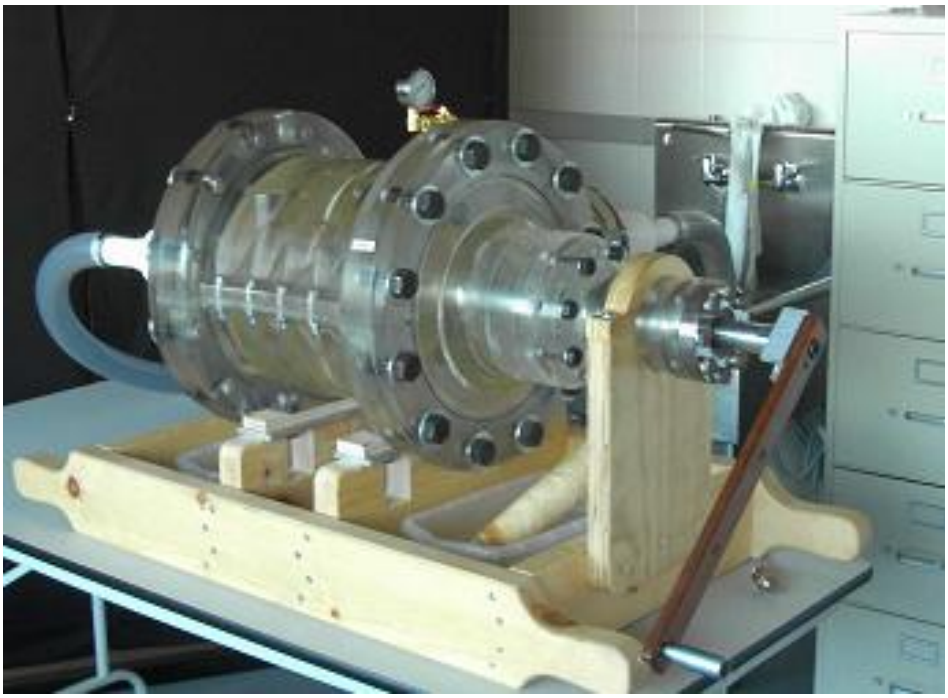

Figure 2.5 Acrylic model to show the interior design and working principal of TurboPiston Pump

2.2.1 Pattern

In casting, a replica of the part to be cast, called the pattern, has to be made in order to make a mold (section 2.2.2) of which molten metal or other casting material will be poured into. The pattern is made out of a material specific to the type of casting that will be done. For instance, in sand casting, the pattern is often made of wood, plastic, or other materials. While in investment casting, the pattern is often made of wax so it can be melted out and replaced with the casting material.

The design of a pattern has many considerations that must be taking into account such as contraction allowance. When a part is cast with molten materials at elevated temperatures, the casting will shrink upon solidification and cooling. Thus, to compensate for the shrinkage of the casting, the pattern must be made large so the part will shrink to the desired size. Furthermore, after casting, other finishing processes are often done to the casting such as machining to the specified tolerance. The patterns for the TurboPiston Pump made by JRB Innovation and were fabricated using wood. However, for the casting of the 12" acrylic model, shrinkage does not have to be taking into account because when the liquid acrylic resin cures, shrinkage is negligible. Figures 2.6 and 2.7 show the housing patterns for the 12" version of the TPP.

Figure 2.6 Acrylic TPP pattern split in half for making casting mold

Figure 2.7 Acrylic TPP pattern

Draft allowance is another consideration that needs to be accounted for. After packing the mold material around the pattern, the pattern needs to be pulled out. In doing so, the mold can often be damaged if the pattern is not properly and carefully removed. In an effort to help remove the pattern, draft is often incorporated on the pattern itself. Draft is when the pattern is slightly tapered so when removed, the pattern doesn't continuously slide against the mold walls.

2.2.2 Mold

The mold is an inverse pattern of the part desired to be made. In general, molds are usually made of sand or similar material for casting of metals because it can withstand the high temperatures of the material being cast. Figure 2.8 shows the cope and drag of a silicon mold used for casting the TurboPiston Pump casing. Silicon was used for the casting of the acrylic TPP because of its flexibility when removing the casting and also because the cured acrylic doesn't stick to the rubber mold. The acrylic piston rotor mold can be seen in Fig. 2.9 with the cast pistons next to the mold.

Figure 2.8 Acrylic TPP silicon mold

Figure 2.9 Acrylic TPP piston rotor mold with finished cast rotor

The sands used for metal casting molds are usually silica or a silica mixture with other minerals. The sand should possess good refractory properties such as being able to handle high temperatures without melting or degrading. Other important features of the sand include grain

size and shape of the individual grains. Small grain size allows for better surface finish of the cast part while larger grain size is more permeable to allow for gasses to escape while pouring.

In making the mold, the sand grains are held together by a mixture of water and bonding clay. The bonding clay holds the shape of the mold together while the casting material is being poured in. Besides the sand and binder, additives are sometimes combined with the mixture to enhance properties such as strength and or permeability of the mold.

To form the mold cavity, sand is packed around the pattern for both the cope and drag (top and bottom section of mold) in a container called the flask. The simplest method is to hand ramming the sand around the pattern; however various machines are also available to help in the process of packing. Figure 2.10 shows a typical mold set up.

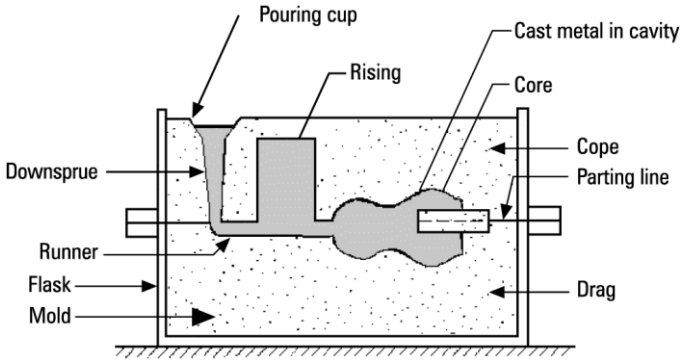

Figure 2.10 Typical mold setup

2.2.3 Casting

There are many different types of casting processes and the type used is dependent on many factors to meet the need of the part being cast. After the cope and drag are made using the pattern, the mold is clamped together and the casting is performed. The process of casting consists of pouring, solidification, and cooling of the cast part. The runner and rising system built into the mold must be designed to deliver liquid into the cavity and provide for a sufficient reservoir of molten metal or other casting material during solidification and shrinkage. Air and gas must be able to escape from the mold or air pockets will be left on the casting, thereby rendering it useless.

When casting the acrylic TPP, the same considerations must be taken into account to those of metal casting. However, solidification time does not play too big of a factor for acrylic

casting as does for metal casting. Figures 2.11 and 2.12 show parts of the 12” acrylic TPP after casting.

Figure 2.11 TPP piston rotor and centrifugal impellor after casting

Figure 2.12 TPP cylinder rotor, piston rotor, and centrifugal impellor after casting

2.2.4 Assembly

The assembly of the TurboPiston Pump consisted of machining and finishing off casting parts such as the runners used to pour the metal. Also, the surfaces had to be smoothed out in areas such as the cylinder where the piston rings would slide back and forth.

On the piston rotor assembly, piston ring groves had to be machined because they are not possible to include into the mold design. Furthermore, the valve retaining ring slots also needed to be machined into the piston heads along with all the bolt patterns for connecting the centrifugal impellor to the piston rotor assembly.

Once the bearings are placed in the bearing carriers on the pump housing and the shafts are installed on the rotors, the pump could be assembled. First the housing end caps are bolted to one side of the pump housing. From there, the cylinder rotor can be installed on the end cap as seen in Fig. 2.13. This will allow for placement of the piston assembly into the cylinder assembly. Finally, the top half of the pump housing can be bolted on to the lower half to complete the assembly of the pump. The final assembly prior to bolting on the upper housing can be seen in Fig. 2.14.

Figure 2.13 Piston rotor ready to be assembled with cylinder rotor

Figure 2.14 Acrylic TPP almost completely assembled

2.3 Metal Demonstration, Testing, and Certification of TurboPiston Pump

The 12” metal TPP was developed after experience learned from fabricating the acrylic TPP model. This metal TPP is used for testing and certification purposes. Since the TPP is so new, it

needs to be tested with regards to an industry standard pump code. Because of its unique design, it does not fall in a particular category of pump test codes. In building a test system for the TPP, evaluations of the different pump codes currently available will aid in determining what should be included in the test system and the TPP code. The 12-inch metal TPP is currently under testing and development. The test system for the 12 inch TPP is designed for laboratory testing in accordance with combination of selected pump test codes, and the components will be sized and selected to achieve accurate and repeatable test results. Suitable components and instrumentation have been sized and selected. Please see (Hotard et al. 2008) for more details.

2.3.1 Testing and Certification

The idea behind using a pump code for testing and certification is to standardize the testing process and eliminate any potential for error and inaccuracy in the pump performance. The test system for the 12 inch laboratory testing pump was designed by a group of undergraduate mechanical engineering students [Hotard et al. 2008] in accordance with a selection of pump test codes from ASME, ISO 5198, and ANSI/HI. Based on the codes selected to make a TPP code, components were sized and selected to achieve accurate and repeatable test results.

In an effort to save space and plumbing, a recirculation system was chosen for the test layout. The size of the recirculation tank is based on the amount of water it can hold and the flow rate of the pump. The tank should be able to accommodate a minimum of two minute water recirculation time. Thus, for the 12 inch TPP with approximately 700 gpm, the recirculation tank should be capable of storing at least 1400 gallons.

To test the net positive suction head required, ($NPSH_R$), there are three main options available to impose a pressure drop at the suction side of the pump. The first option is to install a throttling valve on the suction side of the pump that can be opened and closed to increase and decrease the net positive suction head actual ($NPSH_A$) to the pump respectively. The second option is to modulate the pressure in the recirculation tank using a vacuum pump and a compressor. This option does not require the use of a throttling valve, and therefore imposes fewer in efficiencies and reduces the risk of premature cavitation at a throttling valve. The final option is to have a tall recirculation tank in which the suction side of the pump is routed to pull the water out of the top of the tank. As with the second option, there is no need for a throttling

valve on the suction side of the pump, but the water level in the recirculation tank must be able to be modulated by the tester. By lowering the level in the recirculation tank, the pump is then required to lift the water higher which reduces the $NPSH_A$ at the pump inlet. Although the third option is the closest to how a pump is used in real world applications, in order to offer a full scale test, the recirculation tank water level would have to be adjustable over a range of 33 feet. This is the depth of water at which absolute zero pressure is reached. This is not practical for the space which has been allocated for the test rig. Furthermore, the second option requires lots of energy and time to throttle the pump by changing the pressure inside the tank using either a vacuum pump or compressor; therefore, a preliminary test facility based on the design of the first option has been completed. The design diagrams are shown in Figs. 2.15 and 2. 16 and the completed rig is shown in Fig. 2.17. Currently an inlet throttle valve is not installed on the test rig due to funding and the suction pressure is set at a predetermined pressure. Continuous improvement of the test facility is undergoing.

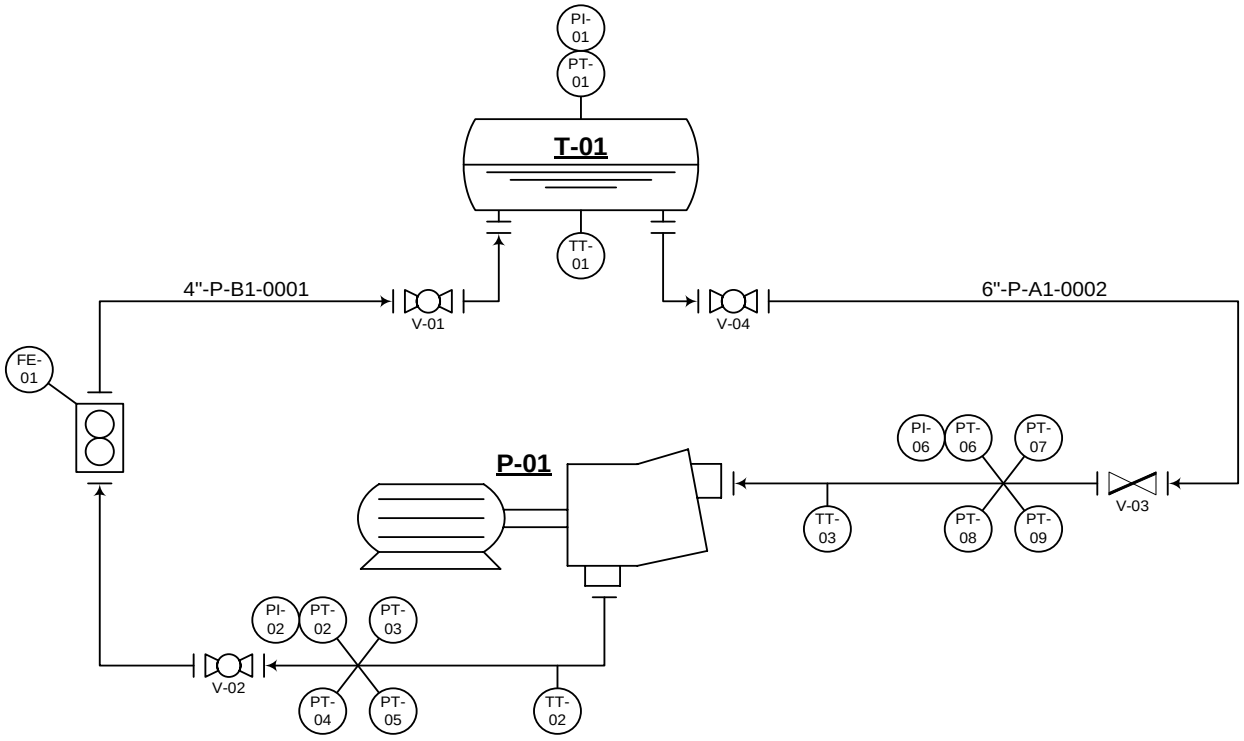

Figure 2.15 Piping and Instrument Diagram for first option of a pump performance test facility

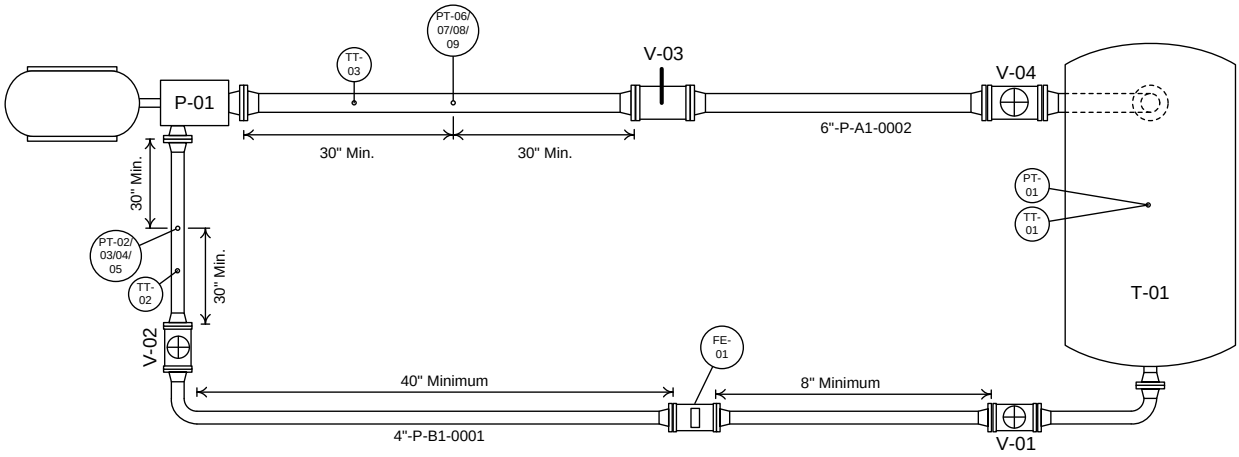

Figure 2.16 Piping Plan for first option of a pump performance test facility

Figure 2.17 Front and side views of a preliminary TPP test layout

Chapter Three

Modifications, Improvements and Testing

In order to improve the TurboPiston Pump and bring it to market, the pump must go through a series of test followed by modifications and improvements. This will help in obtaining a reliable, efficient and quality product to sell to customers.

3.1 Valves

The valves on the TurboPiston Pump are a key component that has gone through multiple design changes over the design and testing phase of the pump. The original valves in the TurboPiston Pump are essentially check valves which only allow fluid to flow in one direction. The opening and closing of the valves are controlled by the flow field through the pump. Ideally a well-design valve will have a large flow area, thus helping to keep velocities to a minimum and will also allow for large particles to flow through for pumping in certain applications.

There are two separate valves that need to be looked at when analyzing the pump itself, namely the intake and discharge valves. The first is the intake valves which are mounted on the pistons of the TPP. The intake valves are the most crucial because they have the lowest pressure head entering them, thus are prime candidates for cavitation. Cavitation occurs when the static pressure of the fluid drops below the fluid vapor pressure. When this occurs, vapor and air bubbles form in the fluid and then collapse on themselves when they flow back into a region of high pressure. This can be devastating on a pump by quickly destroying the valves and other components to render the pump progressively reducing efficiency until it fails. Furthermore, while trying to keep cavitation from happening by using large flow passages, this also reduces any unrecoverable pressure drops through the valves. The pressure drop across the valve is due to friction, entrance losses and exit losses. These losses are proportional to the velocity square of the fluid going through the valve and therefore a large flow area will give a lower velocity through the valves and therefore less pressure drop.

The discharge valves are less crucial because the static head pressure is large compared to that of the inlet valves. Thus cavitation should not exhibit a problem, however in the same manor of the intake valves; they have to allow for large particles to flow through if ingested.

3.1.1 Flapper Valve

The initial TPP valve design called the flapper valve, seen in Fig. 3.1, consists of a rubber disk mounted on the backside of valve body as seen in Fig. 3.2. This design was used on both the intake and discharge, however were problematic during testing of the TurboPiston Pump. It was found through testing that the rubber material would not last very long and would often be shredded after a given time period of the pump running.

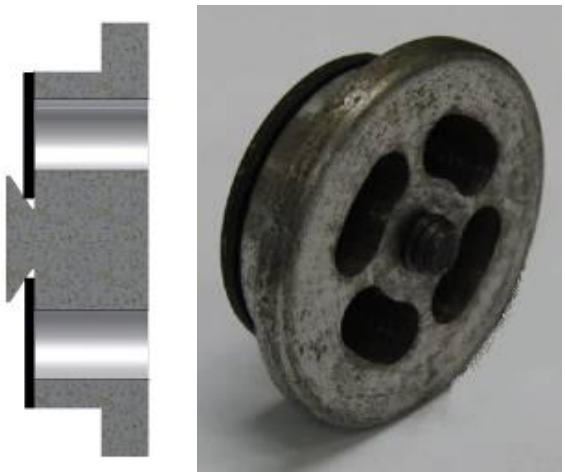

Figure 3.1 Flapper Valve cross section and side view

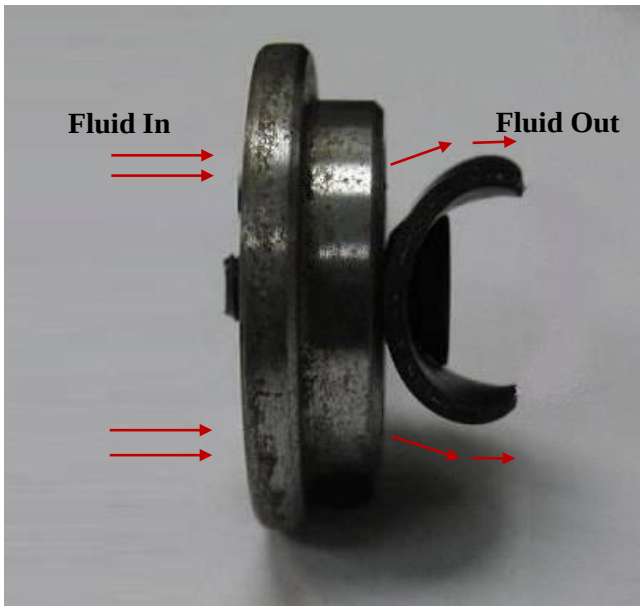

Figure 3.2 Flapper valve opens by flapping back and closes by folding back flat

These valves also possess a small flow area and thus have a large fluid velocity flowing through them. This leads an increased pressure drop across them and may have partially

contributed to the destruction of the rubber flaps. The irreversible pressure loss through a valve is a function of the velocity square, thus it is ideal to keep the velocity small through flow passages to reduce any pressure losses through the pump. This will also help reduce adverse effects attributed to cavitation and vorticites, which also contribute to inefficiencies

Furthermore, these valves were retained in both the piston and the cylinder rotor using c-clips. This method made for easy installment and removal of the valves; however c-clips are not designed to take large side loads as seen on the valves due to the pressure differential acting on the valve. This led to the c-clips bending and eventually failing.

The flapper valve is a good design in that it's very simple in construction and possesses almost no moving parts besides the rubber flap itself. These qualities usually lead to reliability and longevity in products; however the flapper valves as originally used on the TPP needs to be redesigned. If a larger flow area is used and better selection of material/reinforcement is used, this design concept has a lot of potential for success.

3.1.2 Piston Valve

After the many failures encountered during testing of the 12" TurboPiston Pump, it was determined that another valve design should be implemented to continue on with testing. The design agrees upon resemble that of a 4-stroke engine valve, however instead of being controlled by a cam, the valve is controlled only by pressure differentials across the valve face and a return spring. Figure 3.3 shows a cross-section view of the discharge valve and the finished valve after machining.

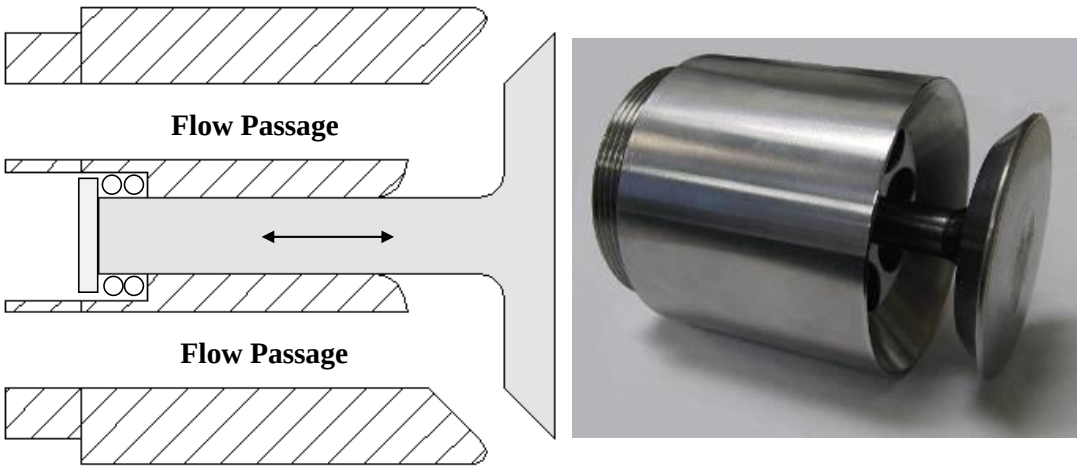

Figure 3.3 Piston valve cross section and side view

This valve was designed from the engineers at Power Engineering in an effort to ramp up testing on the TurboPiston Pump. Few quick tests showed that the flow rates started to level with increased RPM and the flow rates reduces at higher discharge pressures. Both phenomena indicated flow leakages, which prompted initiation of an analytical design analysis of the valve movement.

First intuition of the new valve was the large mass it possessed would cause the valve to have a high inertia. In a valve that should ideally open and close instantaneously, a high inertia would give a slow reaction time to changes in the flow field. A discharge valve with a large reaction time could possibly lead to fluid being sucked back into the cylinder on the expansion stroke, thereby causing a loss in volumetric efficiency. The details of the analysis can be seen in Appendix C.

The valve closing time is proportional to the pressure differential across the valve face which is directly related to the discharge pressure out the TPP. Furthermore, the calculated valve closing time is compared to that of the piston stroke time to give a percentage of how long the valve is open while the piston is moving back on the expansion stroke. Since the piston stroke time varies with the rpm of the pump, increments of 100 rpm were used to see how the percentage of time the valve is open on the expansion stroke increases as the rpm increases. It is noticed that the amount of time the valve remains open during the expansion stroke ranges from as low as 3.5% at 100 rpm and zero psi discharge pressure all the way up to 90% at 2600 rpm with zero psi discharge pressure. This long duration at higher rpm allows unwanted back flow of water into the cylinder, which will cause a loss in volumetric efficiency.

In an effort to reduce the valve closing time, a number of modifications can be made. This include increasing the spring constant, however this will have negative effects by creating more resistance when the valve tries to open. Another much more effective modification would be to reduce the moving valves mass by, for example, fiberglass reinforced composite materials. A reduction in weight will lower the inertia of the valve and allow the response time to increase substantially.

3.2 Valve Test Experiment

One of the main moving parts on the TurboPiston Pump is the valves on both the intake and discharge of the cylinders. Each valve in the pump reciprocates at the same rate of the pump,

and for a pump that runs at up to 3600 rpm, this can put a lot of wear and tear on the valve. Furthermore, since the TurboPiston Pump can achieve a high volume flow rate, the velocities going through the valves may become very high. The high velocities going through the valves relates back to efficiency loss in the form of both pressure losses through friction and energy dissipation through vorticity generation. The pressure loss through the valves is on the order of velocity square, thus it is best to keep the flow area large to maintain a low velocity through flow passages.

3.2.1 Valve Flow Simulation

Although many different valves are being tested on the TurboPiston Pump, the flapper valve design was chosen to be tested in the laboratory to further study the flow characteristics around the valve and the valve motion itself. In order to do this for the intake valve, both the suction stroke and piston stroke have to be simulated.

There are many ways in which this can be done. One such ways is by making a transparent piston and cylinder assembly with the flapper valve installed on the intake region. When the piston moves back on the suction stroke, fluid will be sucked in through the intake flapper valve. Likewise, on the discharge stroke, the intake flapper valve will close, thus simulating the condition when it is exposed to the high discharge pressure in the cylinder. Eventually, the fluid in the cylinder will flow out another valve to a dump tank. Another way to achieve the suction and discharge strokes of the TPP is to use a Diaphragm pump. The diaphragm pump works in the same manner as connecting a piston to the test section except the plumbing will be different for the experiment. Figure 3.4 shows a cross section of a diaphragm pump with arrows showing flow directions for both the suction and discharge stroke. The use of a diaphragm pump was chosen for this experiment due to its simplicity and setup.

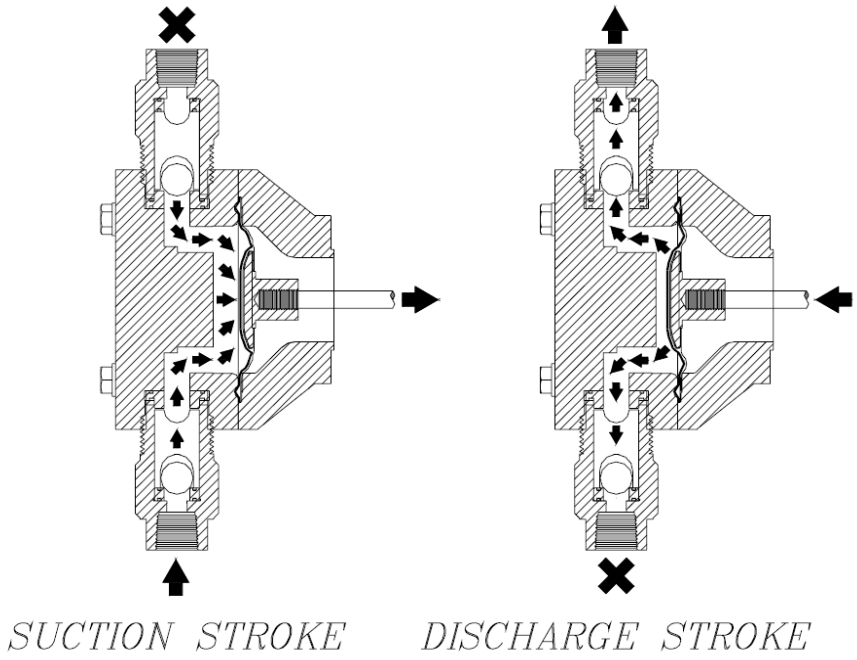

Figure 3.4 Diaphragm pump cross section and its working cycle

3.2.2 Experiment Design

In order to properly design the experiment to best simulate what the valve will see while operating, both low pressure and high pressure will have to be simulated using the diaphragm pump as seen in Fig. 3.7. However, full simulation of all the forces and pressures cannot be done easily in the lab condition with an easy access for flow visualization and instrumentation, and thus some areas were compromised. For instance, while the TPP is running, the fluid flowing through the valve also experiences centrifugal force due to the rotational motion of the pump. This would not be practical to implement in an experiment due to the complexity it would introduce. Figure 3.5 shows a layout of the valve simulation experiment along with the flow path through the plumbing.

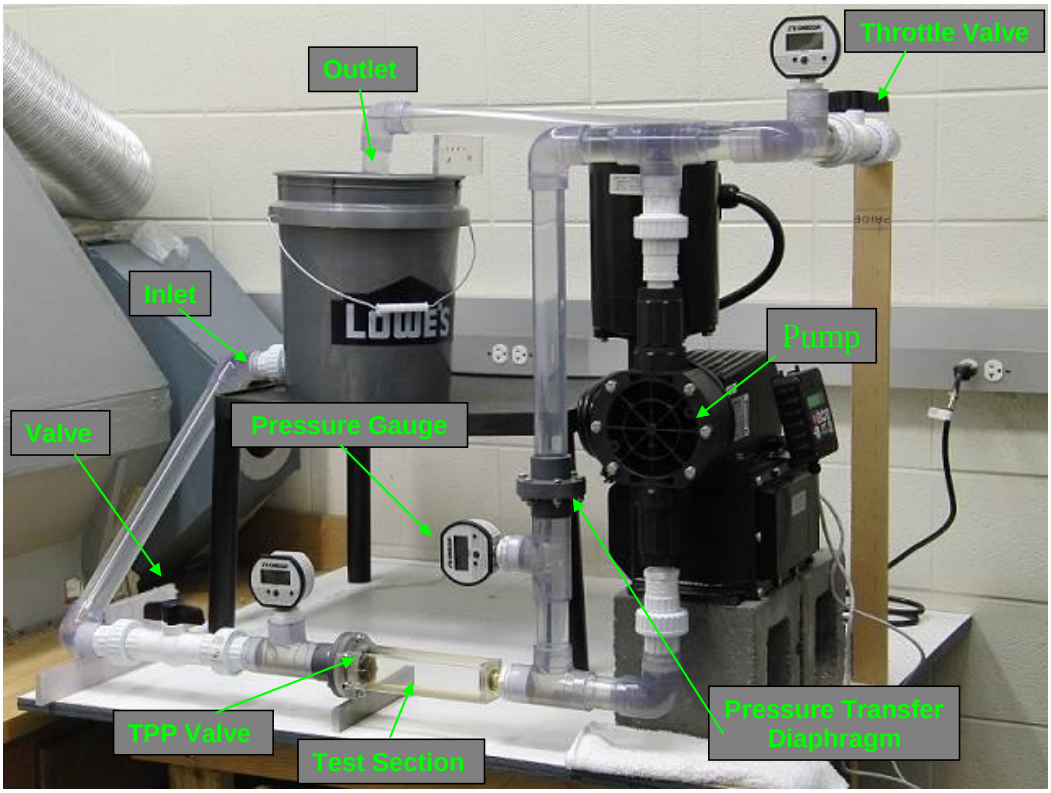

Figure 3.5 Flapper valve experiment layout.

Due to the nature of the flapper valve, it's not clear what the valve flap motion will be like while the TurboPiston Pump is running. It was decided to build the experiment out of clear PVC pipe and Acrylic to allow for flow visibility throughout the whole experiment. This allows for visual verification of any bubbles present throughout the experiment plumbing and also allows for clear viewing of the flapper valve motion while running. For the actually test section, a square tube is used so the valve is not visually distorted when viewing through the side walls. Furthermore, it allows for both, a Phase Doppler Particle Analyzer (PDPA) to be used for flow field studies, or the use of a laser screen for visualization of the flow field. The material for the square section is acrylic due to clear PVC square tubing not being available on the market. Figure 3.6 shows a picture of the test section with the valve holding flange.

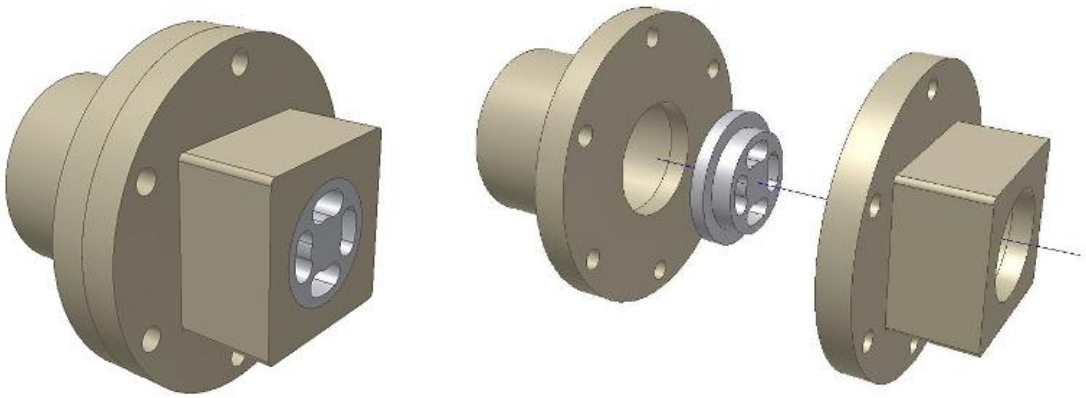

Figure 3.6 Valve test section holding flange

Simulation of the high pressure seen on the intake valve while piston is on the discharge stroke is simulated using a rubber diaphragm. The setup is at the discharge of the diaphragm pump where high pressure flow travels back into the return bucket; however the pressure wave from the pump is allowed to pass through the diaphragm while keeping flow from traveling through. The pressure wave then travels back to the test section to simulate the high pressure on the valve.

In order to generate high pressure, the setup has a PVC ball valve at the diaphragm pump discharge end. The valve can then be opened and closed to the desired discharge pressure. Just upstream of the valve is a digital pressure gauge as seen in Fig 3.8, to display the pressure generated due to resistance through the ball valve.

Figure 3.7 Flapper valve diaphragm pump

Table 3.1 Diaphragm pump specifications

Diaphragm Pump Specifications		
Flow Rate (GPH)	**Pressure Range (psig)**	**Power (HP)**
0 - 108	0 - 90	0.5

Figure 3.8 Omega digital pressure gauge

Table 3.2 Omega pressure gauge specifications

Pressure Gauge Specifications		
Pressure Range	**Accuracy**	**Temperature Range**
0-500 psig	± .25% FSO	-4 to 185 F

3.2.3 Experiment Setup and Testing

After instillation of the TurboPiston Pump flapper valve in the test flange, a sealing o-ring is placed in between the two flanges that hold the valve in and then are bolted together. The test section can then be installed on the experiment for testing. Before testing can proceed, the experiment has to be filled with water. This is done by filling the water holding tank up with water and allowing it to flow through the system. Air has to be bled out certain sections such as below the diaphragm that transmits pressure back to the test section. This is done by loosening the bolts on the diaphragm flanges and allowing air to bleed out until water starts to drip out. The bolts are then tightened up to seal any further leaking.

Once the experiment is properly filled with water, all the pressure gauges should be turned on. Furthermore, ensure that all ball valves on the experiment are in the open position. Running the experiment with a valve completely closed can result in major damage of the experiment or diaphragm pump. The diaphragm pump then needs to be turned on by plugging it into a wall socket. This will turn on the diaphragm pump control unit. Before running the pump, one should bring the flow rate down to zero. The pump can then be turned on and slowly increase the flow rate using the controller.

When the pump is running at the desired frequency, the ball valve on the discharge side of the diaphragm pump can slowly be closed to generate resistance in the system. The resistance will build up pressure to simulate the high pressure seen on the TPP valve when running. When one closes the ball valve, carefully watch the pressure gauge ensure the pressure does not exceed 100psi. One should also take note that since water is incompressible, pressure build up will happen rapidly with small rotation of the ball valve.

3.2.4 Results

By running the flapper valve experiment, an insight into the flap motion is gained from an otherwise unknown motion. The motion is heavily dependent on the material parameters and

properties such as elasticity, thickness, and disk diameter. Without running a laboratory experiment or by using finite element software, it would otherwise be difficult to know the valve geometry at different flow rates. However, this experiment only gives valve motions for up to 80 RPM of the TPP due to limitations in the diaphragm pump selection.

After running the experiment, it is noticed that the flap does not bend back very much. Instead, the valve flap acts more like a solid disk that pulsates back and forth. This is due to the low flow rate going through the valve along with low inlet pressures. When the pump is turning at a higher RPM, the flow rate and pressure will be much greater and the momentum of the flow will fold the valve back much further. At higher speeds, the large momentum flux passing the valve flap is most likely the reason for the flapper valves failing in the pump. Figure 3.9 shows a picture of the TPP flapper valve while running in the test rig at a speed equivalent to 80rpm on the TurboPiston Pump.

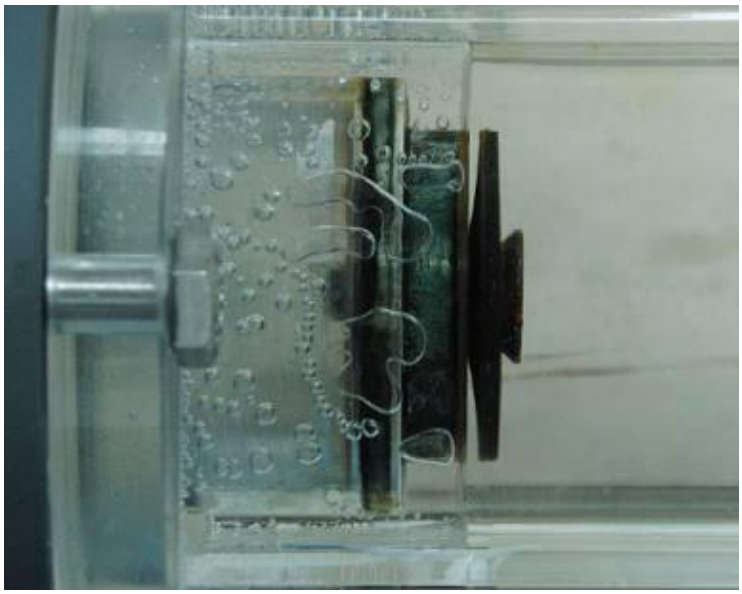

Figure 3.9 Flapper valve fully open in test rig at equivalent speed of 80 rpm on TPP.

To visualize the flow around the flap as fluid passes through, small particles were introduced into the flow. A laser was then used with a cylindrical lens to create a plane of light that passes through the test section. When the particles pass through the laser screen, light refracts off the surface and allows one to see the particle. The particles used in this experiment were made of oak wood dust for simplicity. Oak wood has a density of approximately 50 lbs/ft^3, which is close to that of water. Oak particles were observed to stay suspended in water for over 8 hours, and thus it was assumed to be good for use as the particle medium.

When running the experiment with the laser screen, a high speed camera (EX-FH20) was used to capture particle stream lines. By looking at multiple frames, large vortices develop directly behind the valve. One compromise made when designing the flapper valve experiment was the close proximity of the walls near the valve exit. Figure 3.10 shows multiple frames of the flapper valve while testing with the laser screen.

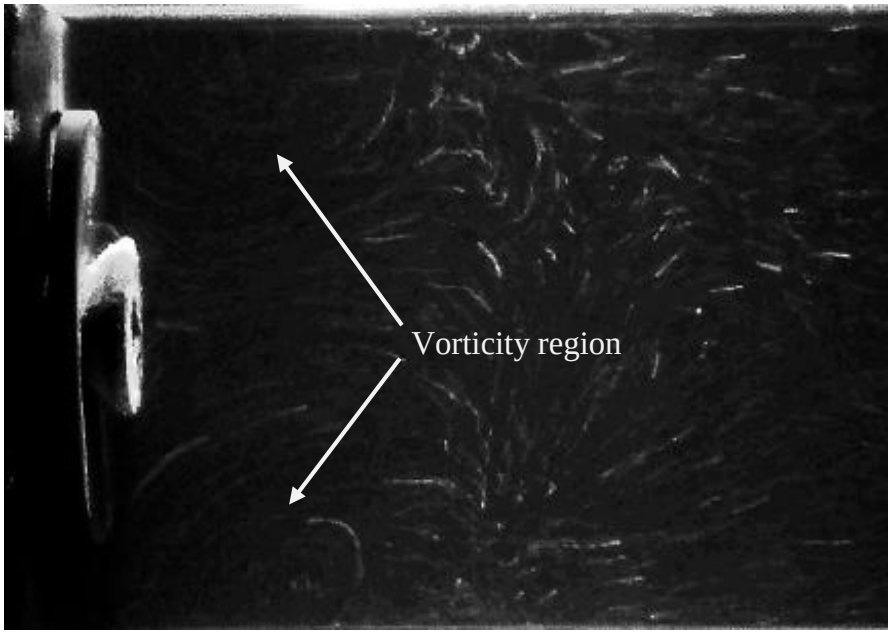

Figure 3.10 Flapper valve in test rig with particles and laser screen. Vorticities can be seen behind valve.

3.3 Piston Rings

The piston rings used on the TurboPiston Pump have to be made to withstand the wear and tear due to high pressure, constant reciprocating motion and side wall forces. In order to achieve this, extensive material research along with a lot of testing and various designs of the piston rings must be made. Unlike conventional metal piston rings found on engines and pumps, the TPP uses plastic and plastic composite rings which help deform and reduce wear to the cylinder surface.

Although a lot of testing has been done on the piston material and design, the rings are still having problems withstanding all the forces introduced while the pump runs. One of the main causes of failure is believe to be due to the nature of the TPP design itself.

The TurboPiston Pump was designed where the input rotor transmits rotation and associated power to the output rotor through the pistons themselves. This leads to a major

problem because the contact point between the input and output rotor is only through the piston rings. This means that all the torque is being transmitted through the rings while they are also in constant reciprocating motion. The side load being applied to each ring is approximately 135lbs due only to the torque transmitted through the shafts when the pump is running at full power. Pictures can be seen in Fig. 3.9, where the piston rings are damaged by breaking at the edges. This is most likely due to the constant side loads and the reciprocating motion.

Figure 3.11 Piston ring damage

One of the solutions to this problem is by finding a material capable of handling the forces present and a material with a high endurance limit to help keep maintenance to a minimum. Another approach that could be done would require a major design change. Since the two rotors are at an offset angle, two bevel gears could be used. This would allow all the power to be transmitted through the metal teeth of the gears which are much more capable of handling the power seen inside the TPP.

In conclusion, the piston rings are still being researched for better materials and designs. However, the most promising solution will most likely be through both, design changes and material selection in the piston rings. This may include changing how many rings are used per a piston, shape, and multiple materials on each piston.

3.4 Centrifugal Impeller

A typical centrifugal impellers purpose is to increase the pressure of a fluid. This is done by rotating a fluid through an impeller and imparting kinetic energy to the fluid using centrifugal force. At the exit of the impeller, the fluids kinetic energy is much greater than at the inlet. The kinetic energy can then be converted into pressure energy by using a diffuser.

The pressure at the output of a centrifugal impeller is very useful because the rise in static head pressure allows for higher velocities through small passages without inducing cavitation. The TurboPiston Pump takes advantage of this by implementing a centrifugal impeller before entering the intake valves on the pistons. This allows for the pump to obtain high flow rates without the damaging effects of cavitation. This is especially important and advantageous for a suction type piston motion. This is the reason that TPP doesn't need a charge pump that is a fixture for traditional high-pressure piston pumps.

The TPP's current centrifugal impeller design can be optimized for improved efficiency and a higher discharge pressure through careful analysis. Although the current design works, the impeller has a single channel that flows to each cylinder within the pump without much design work put into creating a proper vane profile or inlet and outlet angles. By using a properly designed vane profile, the impellor efficiency can be increase along with a greater head pressure entering the piston cylinders.

Chapter Four

Computational Fluid Dynamic Modeling

Computational Fluid Dynamics, better known as CFD, is often employed in the branch of fluid mechanics to solve complex fluid problems using software to perform millions of calculations involving fluids interacting with surfaces defined by the boundary conditions. One of the main objectives of this research is to study the flow through the valves on the TurboPiston Pump.

To aid in understanding and analyzing the flow within the TurboPiston Pumps valves, Ansys Fluent 12.0 is used to do an in-depth study of the flow structure and valve mechanics. The initial valves employed on the pump are called flapper valves. These valves use a rubber disk that folds back when fluid flows through the valve, and seal against the valve face when fluid tries to flow in the opposite direction. After many problems with the rubber valve material failing at higher pressure and flow rate, another type of valve was designed and installed on the pump. This type of valve often called the "piston valve" uses a metal valve that opens and closes similar to that of a car engine valve. The valve opens and closes mainly due to the fluid field around it, however a spring does aid in closing the valve.

Since the valves move and are not under steady state conditions, the valves were simulated in Fluent using a dynamic mesh scheme. This allows the valves to move while running a transient case by re-meshing around the valve as it opens and closes.

4.1 Physical Characteristics of the Problem and Assumptions Made

The physical characteristics of the problem are as follow:

1. Two-dimensional
2. Transient
3. Constant properties

The following are the general assumptions made in this study:

1. No-slip condition (zero velocity) is imposed on wall surfaces.

4.2 Governing Equations

The equations for conservation of mass, conservation of momentum, and energy equation are given as:

$$\nabla \cdot \left(\rho \vec{v}\right) = S_m \tag{4.1}$$

$$\nabla \cdot \left(\rho \vec{v} \vec{v}\right) = -\nabla p + \nabla \cdot \left(\overline{\overline{\tau}}\right) + \rho \vec{g} + \vec{F} \tag{4.2}$$

$$\nabla \cdot \left(\vec{v}(\rho E + p)\right) = \nabla \cdot \left(\lambda_{eff} \nabla T - \sum_j h_j \vec{J}_j + \left(\overline{\overline{\tau}}_{eff} \cdot \vec{v}\right)\right) \tag{4.3}$$

where λ_{eff} is the effective conductivity ($\lambda+\lambda_t$, where λ_t is the turbulence conductivity) and J_j is the diffusion of species j.

The stress tensor $\overline{\overline{\tau}}$ is given by

$$\overline{\overline{\tau}} = \mu\left[\left(\nabla \vec{v} + \nabla \vec{v}^T\right) - \frac{2}{3}\nabla \cdot \vec{v} I\right] \tag{4.4}$$

where μ is the molecular dynamic viscosity, I is the unit tensor, and the second term on the right-hand side is the effect of volume dilatation. The first three terms on the right-hand side of equation (4.3) represent heat transfer due to conduction, species diffusion, and viscous dissipation. The energy E is defined as

$$E = h - \frac{p}{\rho} + \frac{v^2}{2} \tag{4.5}$$

where h is the sensible enthalpy and for incompressible flow and is given as

$$h = \sum_j Y_j h_j + \frac{p}{\rho} \tag{4.6}$$

Y_j is the mass fraction of species j and

$$h = \int_{T_{ref}}^{T} c_{p,j} dT \tag{4.7}$$

where T_{ref} is 298.15 K.

4.3 Turbulence Model

The velocity field in turbulent flows always fluctuates. As a result, the transported quantities such as momentum and energy fluctuate as well. The fluctuations can be small scale and high frequency, which is computationally expensive to be directly simulated. To overcome this, a modified set of equations that are computationally less expensive to solve can be obtained

by replacing the instantaneous governing equations with their time-averaged, ensemble-averaged, or otherwise manipulated to remove the small time scales. However, the modifications of the instantaneous governing equations introduce new unknown variables. Many turbulence models have been developed to determine these new unknown variables in terms of known variables. General turbulence models widely available are:

a. Spalart-Allmaras
b. k-ε models:
    - Standard k-ε model
    - RNG k-ε model
    - Realizable k-ε model
c. k-ω model
    - Standard k-ω model
    - Shear-stress transport (SST) k-ω model
d. Reynolds Stress
e. Large Eddy Simulation

The standard k-ε turbulence model, which is the simplest two-equation turbulence model, is used in this simulation due to its suitability for a wide range of wall-bound and free-shear flows. The standard k-ε turbulence is based on the model transport equations for the turbulence kinetic energy, k, and its dissipation rate, ε. The model transport equation for k is derived from the exact equation; however, the model transport equation for ε is obtained using physical reasoning and bears little resemblance to its mathematically exact counterpart.

The standard k-ε turbulence model is robust, economic for computation, and accurate for a wide range of turbulent flows. The turbulence kinetic energy, k, and its rate of dissipations, ε, are calculated from the following equations:

$$\frac{\partial}{\partial x_i}(\rho k u_i) = \frac{\partial}{\partial x_j}\left[\left(\mu + \frac{\mu_t}{\sigma_k}\right)\frac{\partial k}{\partial x_j}\right] + G_k + G_b - \rho\varepsilon - Y_M + S_k \tag{4.8}$$

and

$$\frac{\partial}{\partial x_i}(\rho \varepsilon u_i) = \frac{\partial}{\partial x_j}\left[\left(\mu + \frac{\mu_t}{\sigma_\varepsilon}\right)\frac{\partial \varepsilon}{\partial x_j}\right] + C_{1\varepsilon}\frac{\varepsilon}{k}(G_k + C_{3\varepsilon}G_b) - C_{2\varepsilon}\rho\frac{\varepsilon^2}{k} + S_\varepsilon \tag{4.9}$$

In equations (4.8) and (4.9), G_k represents the generation of turbulence kinetic energy due to the mean velocity gradients and is defined as

$$G_\kappa = -\overline{\rho u_i' u_j'} \frac{\partial u_j}{\partial x_i} \tag{4.10}$$

G_b represents the generation of turbulence kinetic energy due to buoyancy and is calculated as

$$G_b = \beta g_i \frac{\mu_t}{\mathrm{Pr}_t} \frac{\partial T}{\partial x_i} \tag{4.11}$$

Pr_t is the turbulent Prandtl number and g_i is the component of the gravitational vector in the i-th direction. For standard k-ε model the value for Pr_t is set 0.85 in this study. The coefficient of thermal expansion, β, is given as

$$\beta = -\frac{1}{\rho}\left(\frac{\partial \rho}{\partial T}\right)_p \tag{4.12}$$

Y_M represents the contribution of the fluctuating dilatation in compressible turbulence to the overall dissipation rate, and is defined as

$$Y_M = 2\rho\varepsilon M_t^2 \tag{4.13}$$

where M_t is the turbulent Mach number which is defined as

$$M = \sqrt{\frac{k}{a^2}} \tag{4.14}$$

where $a \left(\equiv \sqrt{\gamma RT}\right)$ is the speed of sound.

The turbulent viscosity, μ_k, is calculated from equation

$$\mu_k = \rho C_\mu \frac{k^2}{\varepsilon} \tag{4.15}$$

The values of constants $C_{1\varepsilon}$, $C_{2\varepsilon}$, C_μ, σ_k, and σ_ε used are

$C_{1\varepsilon} = 1.44$, $C_{2\varepsilon} = 1.92$, $C_\mu = 0.09$, $\sigma_k = 1.0$, $\sigma_\varepsilon = 1.3$

The turbulence models are valid for the turbulent core flows, i.e. the flow in the regions somewhat far from walls. The flow very near the walls is affected by the presence of the walls. Viscous damping reduces the tangential velocity fluctuations and the kinematic blocking reduces the normal fluctuations. The solution in the near-wall region can be very important because the solution variables have large gradients in this region.

. Since dynamic mesh scheme is used in this study, detailed turbulence structure in the near-wall region is difficult to be resolved without using brutal computational power. To simplify the calculation, the near-wall turbulence structure is assumed to follow conventional law-of-the wall behavior. Therefore, wall functions, which are a collection of semi-empirical formulas and functions, are employed to connect the viscosity-affected region between the wall and the fully-turbulent region. The wall functions consist of:

- laws-of-the-wall for mean velocity and temperature (or other scalars)
- formulas for near-wall turbulent quantities

There are two types of wall function: (a) standard wall function and (b) non-equilibrium wall function. The former is employed in this study. The wall function for the momentum is expressed as

$$U^+ = \frac{1}{\kappa}\ln\left(Ey^+\right) \tag{4.16}$$

where

$$U^+ \equiv \frac{U_P C_\mu^{1/4} k_P^{1/2}}{\tau_w/\rho} \tag{4.17}$$

$$y^+ \equiv \frac{\rho C_\mu^{1/4} k_P^{1/2} y_P}{\mu} \tag{4.18}$$

and

κ = von Karman constant (= 0.42)

E = empirical constant (= 9.793)

U_P = mean velocity of fluid at point P

k_P = turbulence kinetic energy at point P

y_P = distance from point P to the wall

μ = dynamic viscosity of the fluid

In the k-ε model, the k equation is solved in the whole domain, including the wall-adjacent cells. The boundary condition for k imposed at the wall is:

$$\frac{\partial k}{\partial n} = 0 \tag{4.19}$$

where n is the local coordinate normal to the wall. The production of kinetic energy, G_k, and its dissipation rate, ε, at the wall-adjacent cells, which are the source terms in k equation, are

computed on the basis of equilibrium hypothesis with the assumption that the production of k and its dissipation rate assumed to be equal in the wall-adjacent control volume. The production of k and ε is computed as

$$G_k \approx \tau_w \frac{\partial U}{\partial y} = \tau_w \frac{\tau_w}{\kappa \rho C_\mu^{1/4} k_p^{1/4} y_P} \tag{4.20}$$

and

$$\varepsilon_P = \tau_w \frac{C_\mu^{3/4} k_p^{3/2}}{k y_P} \tag{4.21}$$

4.4 Dynamic Mesh

The dynamic mesh model in Fluent can be used to model flows where the shape of the domain is changing with time due to motion on the domain boundaries. The dynamic mesh model can also be used for steady-state applications, where it is beneficial to move the mesh in the steady-state solver. Two methods are available for describing the motion of a body within the domain. The first method is done by prescribing the motion of a solid body with time by specifying the linear and angular velocities about its center of gravity. The second method is an un-prescribed motion by which the linear and angular velocities are calculated from the force balance on a solid body. This is done by either using the six degrees of freedom solver (6DOF) or a user defined function (UDF). The update of the mesh is handled automatically at each time step based on the new positions of the boundaries. To use the dynamic mesh model, a starting mesh and the description of the motion of any moving zones in the model is needed. The description of the motion must be specified on either face or cell zones. If the model contains moving and non-moving regions, these regions must be identified by grouping them into their respective face or cell zones in the starting mesh. Furthermore, regions that are deforming due to motion on their adjacent regions must also be grouped into separate zones in the starting mesh.

Three mesh motion methods are available to update the mesh in a deforming region subject to the motion defined at the boundaries.

- Smoothing method
- Dynamic layering
- Local remeshing method

Spring Based Smoothing Method

In the spring-based smoothing method, the edges between any two mesh nodes are treated as a network of interconnected springs. The network of springs is in equilibrium with the initial spacing of the edges before any boundary motion. A force is generated due to a displacement at a given boundary node. The force is proportional to the displacement along all the springs connected to a node. Hook's Law is used to determine the force on a mesh node and can be written as

$$\vec{F}_i = \sum_j^{n_i} k_{ij}(\Delta\vec{x}_j - \Delta\vec{x}_i) \tag{4.22}$$

where Δx_i and Δx_j are the displacements of node i and its neighbor j, n_i is the number of neighboring nodes connected to node i, and k_{ij} is the spring constant (or stiffness) between node i and its neighbor j. The spring constant for the edge connecting nodes i and j is defined as

$$k_{ij} = \frac{1}{\sqrt{|\vec{x}_i - \vec{x}_j|}} \tag{4.23}$$

At equilibrium, the net force on a node due to all the springs connected to the node must be zero. This condition results in an iterative equation such that

$$\Delta\vec{x}_i^{\,m+1} = \frac{\sum_j^{n_i} k_{ij}\Delta\vec{x}_j^{\,m}}{\sum_j^{n_i} k_{ij}} \tag{4.24}$$

Since displacements are known at the boundaries (after boundary node positions have been updated), Eq. 4.28 is solved using a Jacobi sweep on all interior nodes. At convergence, the positions are updated such that

$$\Delta\vec{x}_i^{\,n+1} = \vec{x}_i^{\,n} + \Delta\vec{x}_i^{\,m,\text{converged}} \tag{4.25}$$

where n+1 and n are used to denote the positions at the next time step and the current time step, respectively. The spring-based smoothing is shown in Fig. 4.1.

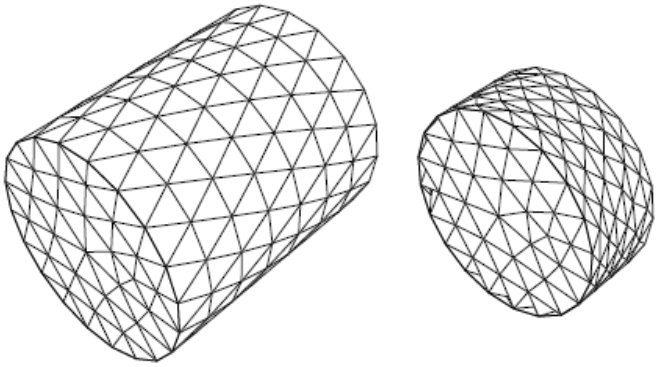

Figure 4.1 Spring based smoothing example of before and after. (From Fluent Manual.)

Laplacian Based Smoothing Method

Laplacian smoothing is the simplest and most commonly used mesh smoothing method. This method adjusts the location of each mesh vertex to the geometric center of its neighboring vertices. This method is computationally inexpensive but it does not guarantee an improvement on mesh quality, since repositioning a vertex by Laplacian smoothing can result in poor quality elements. As a result, the vertex is only repositions if the mesh quality is improved.

Dynamic Layering

In prismatic mesh zones, such as hexahedral and/or wedge, dynamic layering can be used to add or remove layers of adjacent cells to a moving boundary. The cells are added and removed based on the height of the layer adjacent to the moving surface. The dynamic mesh model allows one to specify an ideal layer height on each moving boundary. The layer of cells adjacent to the moving boundary are split or merged with the layer of cells next to it, based on the height (h) of the cells in layer j as seen in Fig. 4.2

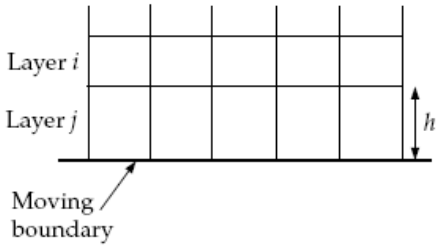

Figure 4.2 Dynamic Layering labeling

Local Remeshing Method

On zones with a triangular or tetrahedral mesh, the spring-based smoothing method is normally used. When the boundary displacement is large compared to the local cell sizes, the cell quality can deteriorate. This will invalidate the mesh, by leading to negative cell volumes and consequently, will lead to convergence problems when the solution is updated to the next time step.

To get rid of this problem, Fluent agglomerates cells that violate the skewness or size criteria and locally remeshes the agglomerated cells or faces. If the new cells or faces satisfy the skewness criterion, the mesh is locally updated with the new cells and the solution is interpolated from the old cells.

Several remeshing methods are available that include local remeshing, local face remeshing (for 3D flows only), face region remeshing, and 2.5D surface remeshing (for 3D flows only). Using the local remeshing method, cells are marked based on cell skewness and minimum and maximum length scales as well as an optional sizing function. Each cell is then evaluated and marked for remeshing if it meets one or more of the following criteria:

- It has a skewness that is greater than a specified maximum skewness
- It is smaller than a specified minimum length scale
- It is larger than a specified maximum length scale

4.5 Flapper Valve Model and Piston Valve Model

The original valves tested on the TPP were flapper valves. They are very simple in design and will keep cost to a minimum by ease of manufacturability and less maintenance. In CFD model, the geometry for the valves is made using Gambit. The best case would be to use a User Define Function (UDF) to define the flapper motion using the rubber properties, geometry and flow field around the flap itself. Two approaches are taken to examine the flow field generated by valve motion. First, a simplified approach is taken by computing the steady-state flow field of the valve opened at several specific positions. They can then be looked at as if they are different snap shots in time as the valve moves. The second approach conducts actual unsteady calculation with the valve moving periodically using dynamic meshing scheme.

The piston valve came about in an attempt to solve the problem with the flapper valves. The valve consists of a stem and valve head that slides back and forth in a sleeve to open and

close. A spring is attached to the valve stem to help keep the valve close until fluid forces the valve open. The only difference between the intake and discharge piston valves on the TPP is the difference between the valve bodies that holds the valve stem as seen in Fig. 4.3. The intake valve has four ½" diameter ports, while the discharge valve has seven 3/8" diameter ports.

Figure 4.3 Inlet (left) and discharge (right) piston valve bodies.

When modeling an object in CFD programs, tradeoffs are often made among computational time, complex geometry, and boundary conditions. For instance, in modeling the discharge valve, a compromise was made to use of a 2-D model rather than a 3-D model. Furthermore, in the pump, the valves are rotating on the rotor; however this rotation is not modeled in the computer model. The rotation will change the flow behavior, especially the pressure distribution, but it is assumed that the effect of rotation will not significantly affect the flow induced by valve motion.

Using the actually discharge valve dimensions, the geometry of the valve was created using Gambit. However, since a 2-D axisymmetrical model is used, the flow channel through the valve must be re-sized to a corrected flow area. This is due to the model being axisymmetrically revolved around a center axis, causing the flow area becomes the shape of annulus, while the actual flow travels through 7 cylinders in a circular pattern around the center axis as seen in Fig. 4.4.

Figure 4.4 Discharge valve flow area of real valve and flow area in 2D space.

The model of the discharge valve was made in Gambit and incorporates a tri-mesh throughout the domain. Since the valve is axisymmetric, only half of the valve is modeled in Gambit. Figure 4.5 shows both a CAD cross section view of the valve and the meshed geometry of the piston, cylinder, valve, and flow discharge area used to solve the domain. To get a better idea of the valve geometry, the domain is mirrored on its axis in Fig. 4.6.

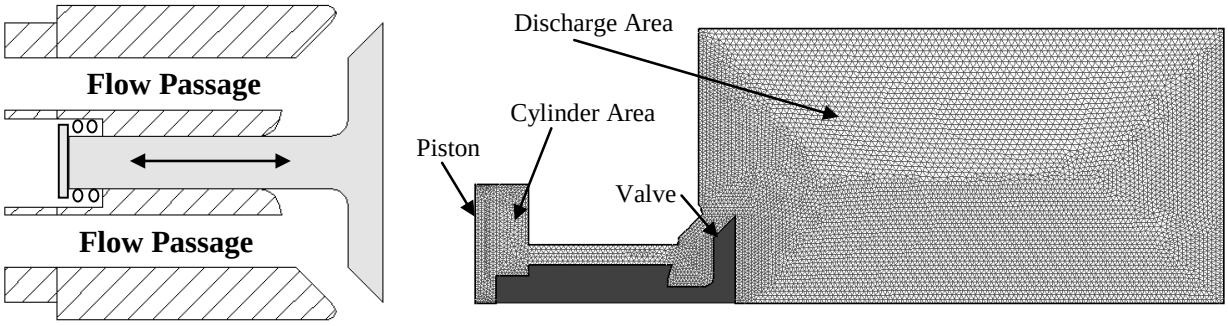

Figure 4.5 CAD model cross section and the axisymmetric computational domain.

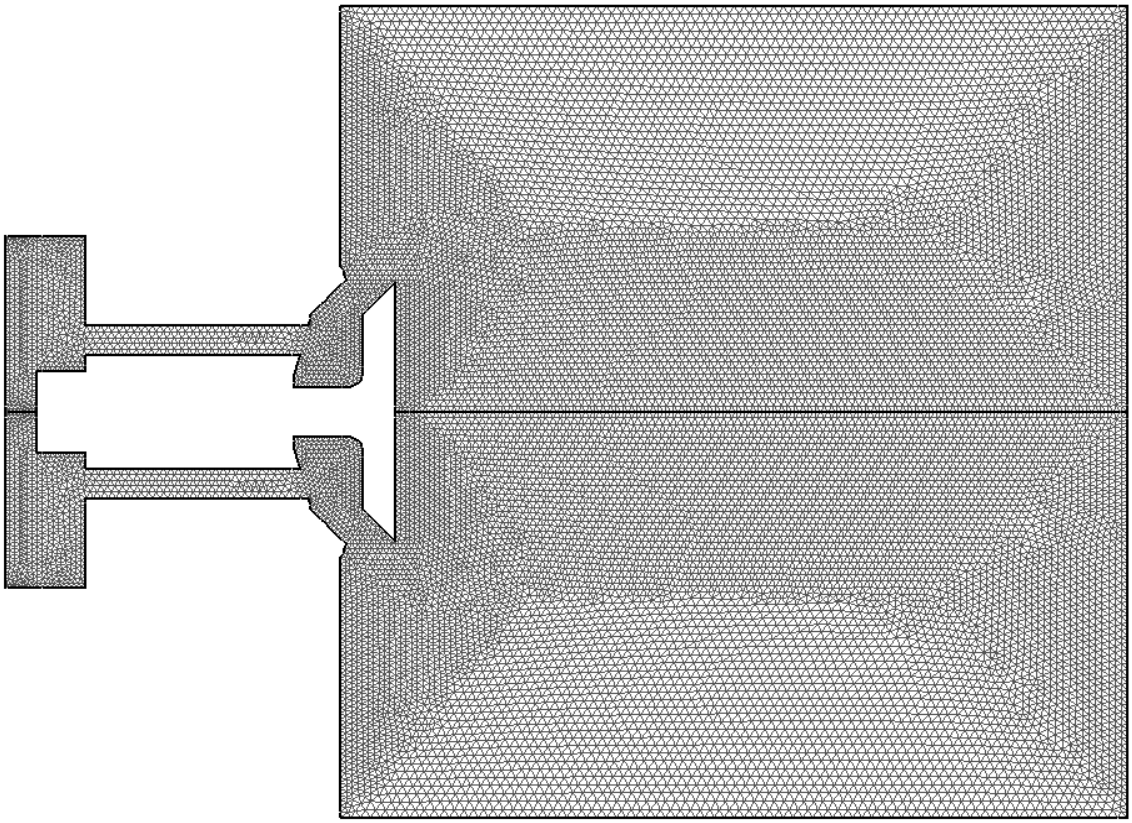

Figure 4.6 Gambit computational model mirrored along axis for easy examination.

The boundary conditions on the discharge valve are set up to simulate those seen in the TurboPiston Pump. At the discharge area of the valve, a Pressure Outlet boundary condition is set up. The pressure outlet boundary condition allows you to specify the static pressure. This allows for different cases to be run with the discharge pressure changing. Three different discharge pressures were selected at 100, 500, and 1000psi.

The volume in the domain increases due to the piston moving from top dead center TDC, to bottom dead center BDC. As seen in Fig 4.5, the piston (modeled as a wall) moves from right to left increasing the cylinder volume. This will cause fluid to flow through the valve and into the cylinder until the discharge valve is fully closed. The speed of the piston is determined by the RPM of the TurboPiston Pump. This is controlled in Fluent using the "In Cylinder" function under dynamic mesh options. Three different RPM ranges of 900, 1800, and 3600 RPM were selected to run in different case files.

In setting up the transient case, first a steady state case is run to determine the flow field just prior to the valve closing. To do this, the piston face is changed to a mass flow inlet where

the mass is determined based of the pump RPM and the outlet pressure. The standard k-ε turbulence model was selected in running the case to simulate turbulent flow in the domain. Furthermore, when setting up the boundary conditions to mass flow inlet and pressure outlet, the turbulent intensity is set to 2%.

In the steady state case, the solution method is set to SIMPLE scheme and first order upwind is used for the spatial discretization. Second order can be used in steady state, however when running the transient model; first order must be used due to limitations of dynamic meshing.

After the steady state solution is run, the transient case can be set up. This is done by first selecting transient under the general tab in the program. Next, the inlet boundary condition needs to be changed from mass flow inlet to a wall. This will allow us to select the inlet wall as a piston to use for the transient case. The pressure-velocity coupling scheme is also changed to Pressure-Implicit with Splitting of Operators (PISO) with the pressure discretization changed to Pressure Staggering Option (PRESTO). In setting up the dynamic mesh, both smoothing and remeshing are selected under the meshing methods.

The discharge valve movement is controlled with the use of a User Defined Function (UDF). The UDF code is attached to the valve geometry and a force balance is applied to the valve every time step to calculate the velocity and distance moved. Furthermore, the mesh update of the region near the valve and the piston are recalculated and updated.

4.5.1 Piston Valve Results

After having no success with the flapper valve during model testing, the piston valve was created to continue on with testing of the TPP. However, as mentioned in chapter 3, problems started showing up when testing the new valve such as flow rates decreasing as RPM increased. After thinking of possible reasons, the large mass and inertia the valve stem and head possess were speculated as prime culprits. To further investigate this possibility and to obtain a complete picture of the physics behind the TurboPiston Pump discharge valve, nine cases were computed to see the full range of operation. The cases change by selecting different boundary conditions on the pump. These include changing the TPP operating RPM and changing the discharge pressure. The location of the valve can be seen in Fig. 4.7.

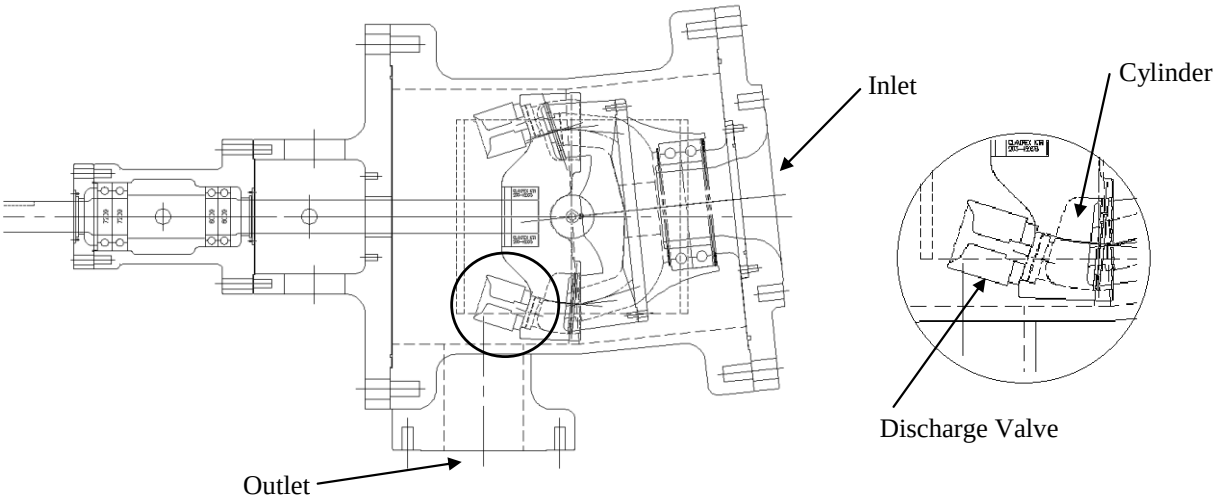

Figure 4.7 Piston valve location in TPP.

The TurboPiston Pump is designed to handle up to 1000psi discharge pressure operating at 3600 RPM. Based on these limits, a 3x3 matrix is made with the pressure ranging from 100, 500, and 1000psi and the angular velocity ranging from 900, 1800, and 3600 RPM. In all cases, the main areas of interest are the valve closing time, fluid backflow into the cylinder, and fluid flow characteristics in the domain. In starting the analysis of the discharge valve, hand calculations were performed to get a baseline engineering estimate of the valve closing time. Using the valve closing time, mass flowing back into the cylinder can be estimated which will correlate to volumetric efficiency loss.

The valve as seen in Fig. 4.5 can be analyzed by using a suddenly applied force (step function) on the valve with a spring and damper. The external force applied to the valve is assumed to be due solely to the pressure differential across the valve face. The governing differential equation of motion describing the valve is shown in Eq. 4.29 from (M.L. James et. al., 1993). Furthermore, Fig. 4.8 shows a simplified free body diagram used for the valve analysis.

Table 4.1 Piston valve and problem data.

Fluid	Water
Valve Weight	.25 lbs
Valve Diameter	2.0 in
Valve Stem Diameter	.375 in
Valve Travel distance "X"	.375 in
Spring Constant "k"	8.9 lb/in

$$\ddot{x} + 2\zeta\omega_n \dot{x} + \omega_n^2 x = \frac{F_0}{m} \tag{4.26}$$

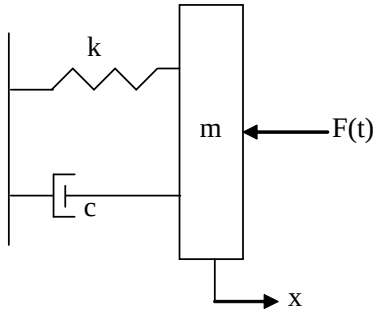

Figure 4.8 Free body diagram of valve system subjected to suddenly applied force.

The solution to Equation 4.26 is

$$x(t) = e^{-\zeta\omega_n t}(A\cos(\omega_d t) + B\sin(\omega_d t)) - \frac{F_0}{k} \tag{4.27}$$

in which $\omega_d = \omega_n\sqrt{1-\zeta^2}$ and $\omega_n = \sqrt{\frac{k}{m}}$

$\ddot{x}$ = acceleration
$\dot{x}$ = velocity
x = distance
ζ = viscous damping factor
ω_n = natural frequency
k = sping coefficient
m = mass
F_0 = suddenly applied force

If the initial conditions are $x_0 = .375$ and $\dot{x} = 0$, constants A and B can be found from Eq. 4.27

$$A = .375 + \frac{F_0}{k} \tag{4.28}$$

and

$$B = \frac{\zeta(.375 + \frac{F_0}{k})}{\sqrt{1-\zeta^2}} \tag{4.29}$$

Furthermore, the viscous damping factor ζ, is due to the drag of the valve moving through the fluid. It is proportional to the velocity square and can be approximated as

$$\zeta = \frac{2}{3}\frac{C_d \rho A |X|}{\pi m} \tag{4.30}$$

Where C_d is the drag coefficient, A is the valve face area, ρ is the fluid density and $|X|$ is the amplitude of the valve motion. In this particular case, the drag coefficient is approximately 2 for a flat plate moving perpendicular to the flow and the amplitude is .375 inches.

Once all the values in the differential equation are known, x(t) can be set to zero and solve for the time it takes for the valve to move from x = .375 to x = 0 as seen in Table 4.2. However, Equation 4.27 is a non-homogeneous differential equation and cannot be solved directly for time. To solve for time, Goal Seek, a function in excel that iterates an unknown variable in an equation until the left hand side of an equation is equal to the right hand side was used. Furthermore, one should note that F_0 is proportional to the pumps discharge pressure.

$$F_0 = P_2 A_2 - P_1 A_1 \tag{4.31}$$

Where $P_2 A_2$ is the average force acting on the outer valve face, and $P_1 A_1$ is the average force acting on the valve back side during the expansion stroke. To solve for the static pressure on the back side of the valve, Bernoulli's equation, equation 4.32, was used with an average fluid velocity. This will then give an average value of the static pressure acting on the valve face to solve for F_0.

$$\frac{P_1}{\gamma} + \frac{V_1^2}{2g} + h_1 = \frac{P_2}{\gamma} + \frac{V_2^2}{2g} + h_2 \tag{4.32}$$

Table 4.2 Analytical valve closing time solution at different discharge pressures.

Discharge Pressure (psi)	Force (lbf)	Valve Closing Time (ms)
0	2.04	10.40
20	4.25	8.54
40	6.46	7.42
60	8.67	6.64
80	10.88	6.07
100	13.08	5.62
200	24.13	4.30
300	35.17	3.61
400	46.22	3.18
500	57.26	2.87
600	68.31	2.63
700	79.35	2.45
800	90.40	2.30
900	101.44	2.17
1000	112.49	2.06

The closing time is assumed to be constant in these calculations because the pressure across the valve face is assumed to be constant at all pump speeds. However, depending on the pump angular velocity, the force acting on the valve will change and thus change the valve closing time. It can be seen in Table 4.3 that as the pump rotating speed increases, the percentage of time the valve is open over the duration of the suction increases as angular velocity increases. This gives an idea of how long the valve is open during the stroke duration and will allow for fluid backflow into the cylinder.

Table 4.3 Ratio of valve closing time to piston stroke time using analytical solution.

Discharge Pressure (psi)	Valve Closing Time (ms)	% of Stroke Valve is Open		
		900 rpm	1800 rpm	3600 rpm
100	5.62	16.86%	33.71%	67.42%
500	2.87	8.60%	17.20%	34.39%
1000	2.06	6.19%	12.38%	24.76%

It must be noted that these calculations are estimates with assumptions that do not necessarily apply to the actual pump. To give a more in-depth study of the closing time and the amount of fluid that is recycled back into the cylinders due to backflow, CFD was used.

After building the model and setting up the boundary conditions as described earlier, the model was used to calculate the nine different cases. The results of the valve closing time compared to that of the hand calculations can be seen in Table 4.4.

Table 4.4 Comparison of analytical and CFD calculation of valve closing time.

		900 rpm		1800 rpm		3600 rpm	
		Hand Calc.	CFD	Hand Calc.	CFD	Hand Calc.	CFD
Pressure (psi)	100	5.6 ms	9.7 ms	5.6 ms	7.0 ms	5.6 ms	4.1 ms
	500	2.9 ms	5.2 ms	2.9 ms	4.6 ms	2.9 ms	3.5 ms
	1000	2.1 ms	3.8 ms	2.1 ms	3.5 ms	2.1 ms	2.8 ms

The results show that the valve closing time is not constant for a given discharge pressure as assumed in the hand calculations and the closing time can deviate up to a maximum of 44% from the CFD calculated closing time.

Next, the fluid mass that recycles back into the cylinder was calculated by integrating the mass flow rate at every time step of CFD calculation. The results are presented in Table 4.5 as a percentage of mass that enters into the cylinder relative to the mass of a full piston stroke. These results are of great value by being able to see how drastic the valve closing time has on the pump performance.

Table 4.5 Comparison of analytical and CFD calculation of mass backflow into cylinder.

		900 rpm		1800 rpm		3600 rpm	
		Hand Calc.	CFD	Hand Calc.	CFD	Hand Calc.	CFD
Pressure (psi)	100	7.44%	20.64%	27.26%	39.56%	77.72%	50.64%
	500	1.98%	6.38%	7.73%	18.47%	28.24%	37.67%
	1000	1.03%	3.51%	4.06%	11.44%	15.51%	27.38%

By making the valve out of lighter material, such as aluminum or composite material, the closing time may be reduced substantially. However, there is still a significant amount of fluid backflow into the cylinder at high angular velocity. Ideally this can be reduced through a different valve design, or by further reducing valve mass. Table 4.6 and Table 4.7 show the valve

closing time and fluid mass recycled back into the cylinder respectively for the 100psi case and all three angular velocities.

Table 4.6 CFD comparison of valve closing time using steel and aluminum valve material.

		900 rpm		1800 rpm		3600 rpm	
		Steel	Aluminum	Steel	Aluminum	Steel	Aluminum
Pressure (psi)	100	9.7 ms	7.2 ms	7.0 ms	5.3 ms	4.1 ms	3.2 ms

Table 4.7 CFD comparison of backflow into cylinder using steel and aluminum valve material.

		900 rpm		1800 rpm		3600 rpm	
		Steel	Aluminum	Steel	Aluminum	Steel	Aluminum
Pressure (psi)	100	20.64%	11.78%	39.56%	21.28%	50.64%	26.02%

To give an idea of how the piston and discharge valve both move to the left during a charging stroke, snapshots were taken every few time steps and shown in Fig. 4.9.

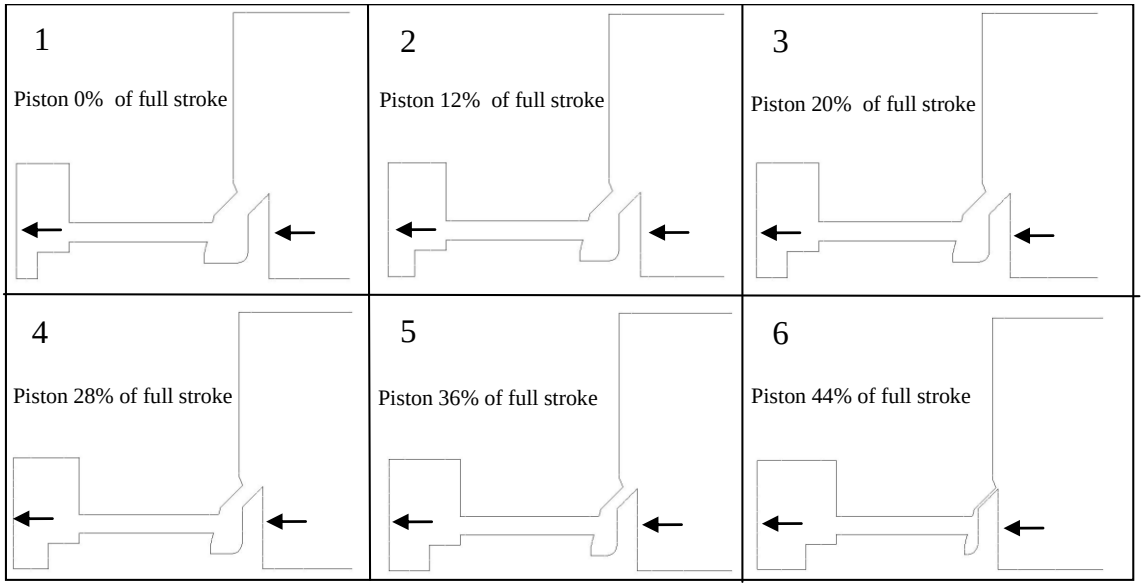

Figure 4.9 Snapshots of piston and valve moving at different time steps.

In looking at the flow field around the valve and piston area for the nine different cases, some cases posses interesting flow fields with turbulence and vorticities. For example in the case running at 1000psi and 900rpm, the piston accelerates from 0 fps at top dead center (0 degrees crank angle) to its maximum speed when the crank angle is at 90 degrees. However, during the

discharge valve closing duration shown in Fig. 4.10, the piston velocity is still very small and thus all the fluid in front (left side) of the valve must be pushed around the discharge valve to make room for the valve. This creates significant entropy through vorticies. The bottom picture in Fig. 4.10, shows the high turbulent intensity formed when the fluid is force to flow behind the valve.

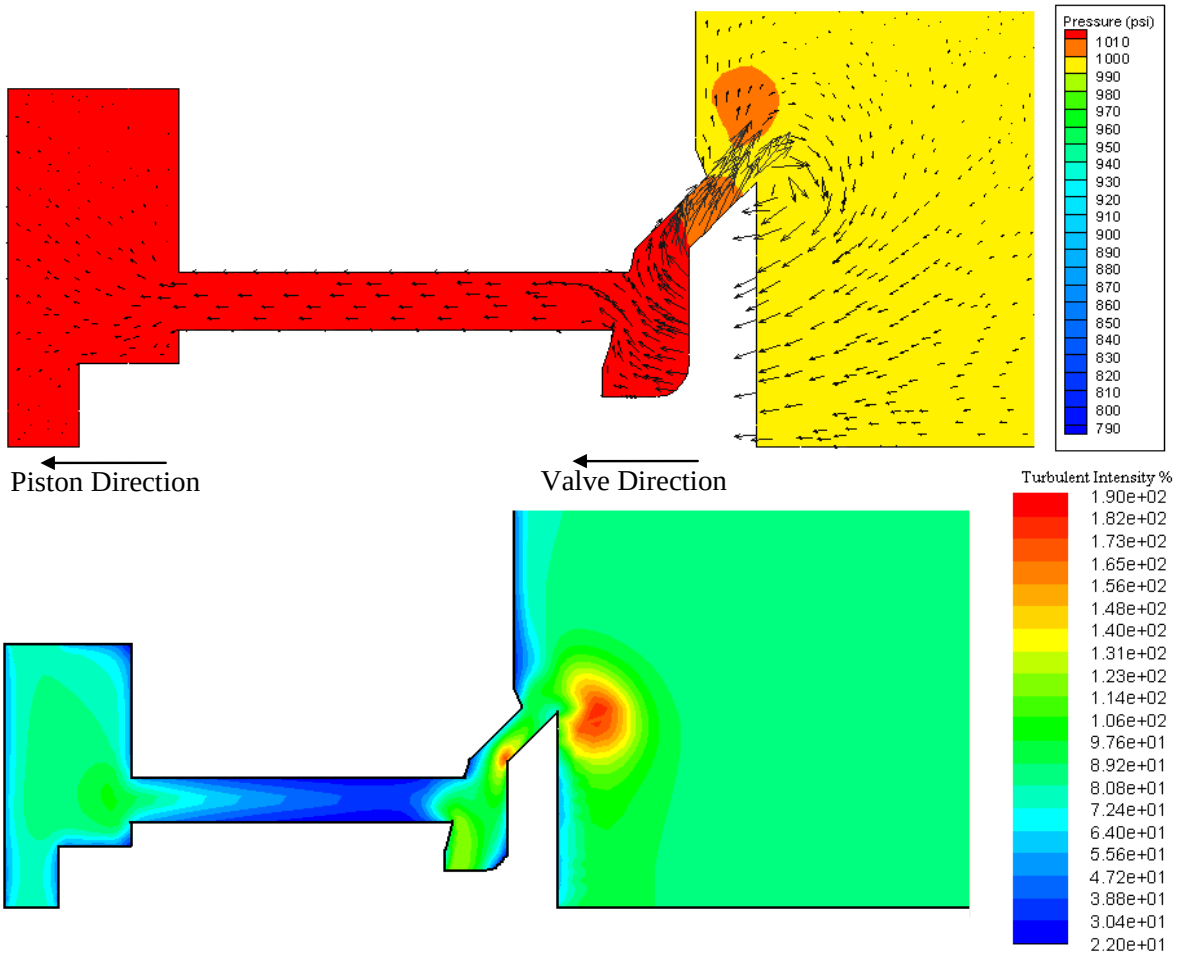

Figure 4.10 Case at 1000psi and 900rpm showing pressure contours with velocity vector overlay (top) and turbulent intensity contours (bottom).

In looking at the case ran at 3600 rpm and 500 psi, the piston (left most boundary) moves much faster than what the discharge valve is moving and an inrush of back flow goes through the discharge valve to fill the cylinder. As the fluid flows past the sharp edge near the cylinder region, a vortex forms behind the edge as shown in Fig. 4.11. The vorticies pull energy from the main flow and produce entropy, thus creating a non recoverable pressure drop. Note that the vortices seen in these 2-D figures are actually vortex tubes surrounding the piston stem in 3-D

axisymmetric configuration. To help increase the pump efficiency, backflow and vortices should be minimized by removing sharp corners.

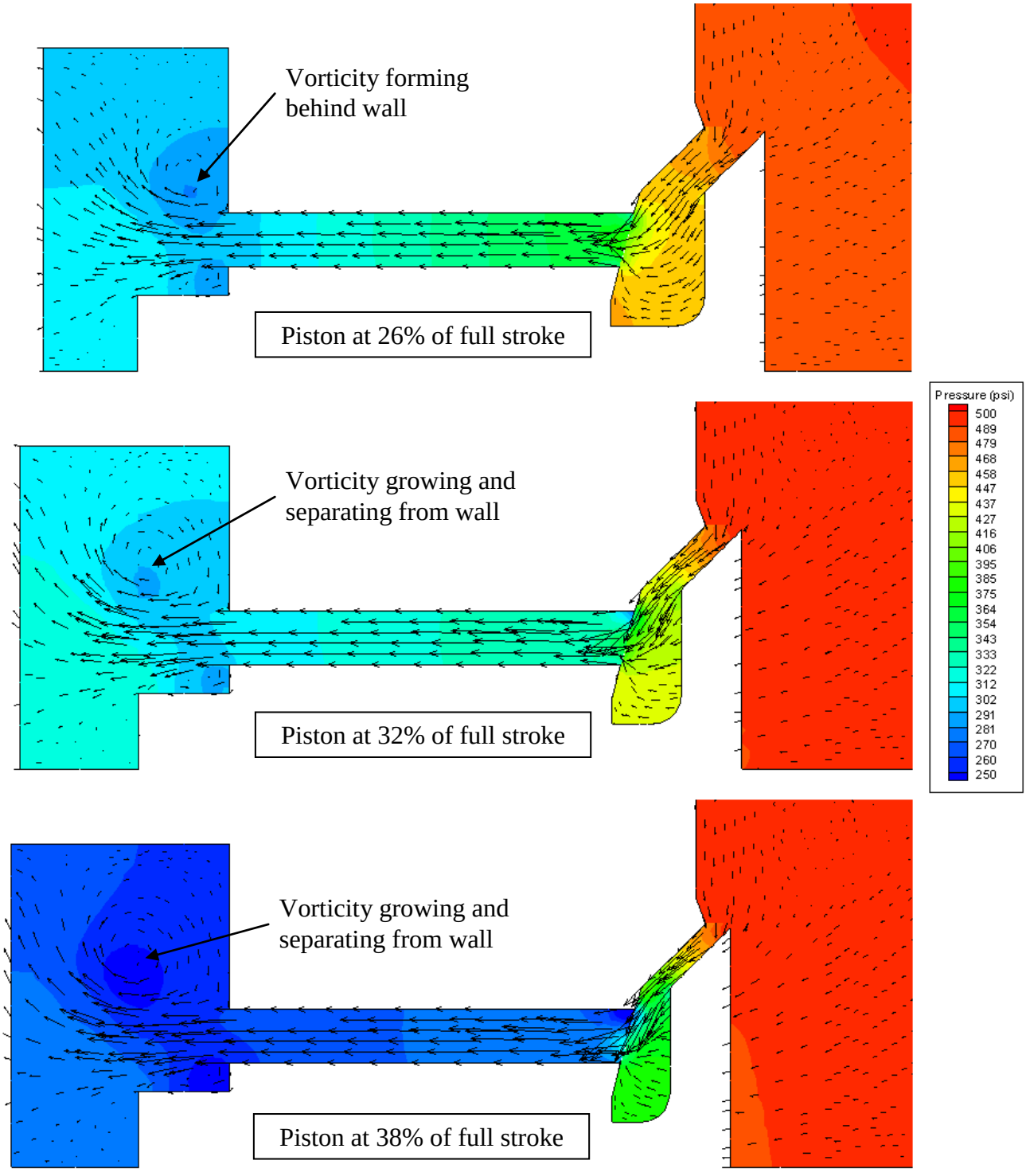

Figure 4.11 Velocity vectors with vortex shedding. Case ran at 500psi and 3600rpm.

Chapter Five

Conclusions and Future Work

In this study, a 12" clear acrylic demonstration model has been made to show the working principle of the TurboPiston Pump. Furthermore, a 12" metal TPP has been made for testing and certification purposes from which potential problems were identified for improvements. Areas thought to cause problems were analyzed using both analytical solutions and through numerical solutions with a CFD program, Ansys/Fluent.

12" Acrylic Demonstration Model and 12" Certification and Testing Metal Pump

The 12" acrylic demonstration model is a valuable tool in allowing one to see the inner working principle of the TurboPiston Pump while running. The acrylic model was fabricated by SR Innovations LLC. The model is able to pump water at a low pressure compared to that of the 12" metal pump used for testing and certification.

In order to bring the TPP to market, the pump has to be rigorously tested to ensure the longevity of parts and to identify areas for improvements. Testing the pump by following strict guidelines set up by professional organizations such as American Society of Mechanical Engineers (ASME) or Hydraulic Institute allows for consistent data while removing the human factor. Currently, no existing test performance code is available for testing TTP. Before an adequate code is developed, the test of TTP tentatively follows the test codes for piston pump and centrifugal pumps. The 12" metal TPP pump is currently being tested at a facility in South Carolina; however, no certifications have been successfully performed to date due to leaking problems with component testing.

Flapper Valve Experiment

The purpose of the flapper valve experiment is to gain a better understanding of how the valve flap moves at reciprocating flow conditions and whether cavitation occurs and to gain an insight into the fluid flow as it passes through the valve. The experimental test rig was built using a diaphragm pump to simulate the reciprocating motion of flow inside the TTP. The rotating effect is not simulated in this experimental arrangement. The flow motion is visualized through the use of a laser screen with particles introduced into the flow stream.

Studying the valve motion, it was found at low frequency the fluid momentum passing through the valve is not enough to bend the flap back, but instead the flap pulsates back and forth

while almost keeping its original disk shape. Furthermore, the experiment allows for two valves to be adjusted, namely the inlet and outlet valve. The outlet valve allows for the buildup of back pressure on the flapper valve while the inlet valve allows for the inlet suction pressure to be decreased. This will allow for cavitation to occur if the static pressure drops below the fluid vapor pressure. However, while adjusting the inlet valve, no cavitation was observed in the test. Due to low frequency and low amplitude of the pulsating flow, this test result doesn't guarantee that there will be no cavitation in the actual operating condition.

When running the experiment with particles introduced in fluid stream, a laser screen was used to view the particle path. As the flapper valve opens, the flow forms a strong vortex directly behind the valve.

Computational Fluid Dynamics of Piston Valve

After the introduction of the piston valve on the TurboPiston Pump, results from testing raised many questions about a loss in flow rate. After contemplating about possible causes, it was strongly speculated that the valve closing time might be the problem, thus, an analysis of the piston valve was deemed necessary. The analysis was first performed by solving analytically a system equation and followed by conducting CFD simulation. The CFD performed also allowed for more detailed study of the transient fluid flow around the valve model.

The analytical hand calculations performed gave a good engineering estimate of the amount of time it takes the piston valve to close and the mass fraction of fluid recycling into the cylinder from the discharge section; however these calculations deviate from the CFD results from 17% to 44%. The CFD results are believed to be more accurate because they better match the pump boundary conditions and takes into account more fluid mechanic details such as vorticities and flow momentum throughout the valve closing time. The results show that nearly 50% of the fluid is recycled into the cylinder from the discharge region when the pump is operating at 3600rpm and 100psi discharge pressure leading to a loss in pump efficiency. By making improvements such as increasing the spring constant on the return spring or more notably changing the valve to a lighter material such as aluminum or reinforced composite materials, the recycled fluid can be reduced by up to 48% of the steel valve as confirmed by CFD calculation.

The flow structure around the valve was different for the nine different cases ran; however, in general two problems seemed to be similar in all cases. One being, the valve is

comparable to that of a flat plate perpendicular to the flow path and thus has a large pressure drop behind the valve causing fluid separation and drag. This leads to a large unrecoverable pressure loss which decreases pump efficiency. Furthermore, the valve possesses sharp edges which create vortices and turbulent flow downstream of the valve. Vorticity generation dissipates energy from the main flow and produces entropy, thus causes a loss in pump efficiency.

Future Work

Based on the present studies, the following are recommended as future work to improve the performance of the TurboPiston Pump:

- Develop a lighter inlet and discharge valve to help reduce valve closing time and fluid recycling into the cylinder.
- Look into better piston ring material to help seal fluid from leaking while also being able to hold up to rigorous environment which they operate in.
- Improve upon the centrifugal impellor to a better hydrodynamic design to increase the head pressure rise by changing the blade profile.

References

1. "Vane pump." Encyclopedia Britannica. 2010. Encyclopedia Britannica Online. 05 Feb. 2010. <http://www.britannica.com/EBchecked/topic/622988/vane-pump>

2. Peter L. Fraenkel. Water Lifting Devices. Practical Action. 2007

3. Kurt J. Lesker. Technical Notes. 2010. Kurt J. Lesker Company <http://www.lesker.com/newweb/Vacuum_Pumps/vacuumpumps_technicalnotes_1.cfm>

4. "Piston-type motors", hydraulicspneumatics.com, 2010. <http://www.hydraulicspneumatics.com/200/TechZone/HydraulicPumpsM/Article/True/6428/TechZone-HydraulicPumpsM>

5. "Pattern (casting)." Wikipedia: The Free Encyclopedia. Wikimedia Foundation, Inc. Aug 2009. Web. 10 April. 2010. <http://en.wikipedia.org/wiki/Pattern_(casting)>

6. Mikell P. Groover. *Fundamentals of Modern Manufacturing*. John Wiley and Sons Inc. 2002.

7. Wanlong Wang, James G. Conley, Henry W. Stoll. *Rapid tooling for sand casting using laminated object manufacturing process*. MCB UP Ltd. 1999.

8. Hotard, E., Nicolaides, J., Serra, N., Tweedley, S., and Wang, T. *Evaluations of Performance Test Codes and Design of Performance Test Facilities for TurboPiston Pumps*. ECCC Report 2008-01. Energy Conversion and Conservation Center. University of New Orleans. January 2008.

9. Merlin L. James, G. M. Smith, J. C. Wolford, P. W. Whaley. *Vibrations of Mechanical and Structural Systems*, Second Edition. Addison-Wesley Educational Publishers, Inc. 1993.

10. ANSYS FLUENT 12.0 User's Guide, January 2009

Appendix

Appendix A

TurboPiston Pump Centrifugal Impellor Pressure Gradient Calculations

This section shows the calculation of the maximum static pressure generated by the TurboPiston Pump centrifugal impellor due to the centrifugal force acting on the fluid as the pump rotates.

Given:

Fluid:	Water
Temperature:	60F
RPM Range:	100-3600
Impellor Inner Radius :	1.5”
Impellor Outer Radius:	4.34”

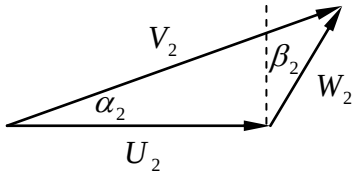

Figure A.1 Exit velocity diagram.

Theoretically the maximum static pressure will be generated in the TurboPiston pump when the flow rate is zero at the exit of the centrifugal impellor (i.e. the static pressure is identical with the stagnation pressure.) Thus, both the absolute velocity, V_2, and the relative velocity, W_2 are zero. This will happen when the piston inlet valve is closed; however once the valve opens, the static pressure will suddenly drop to vacuum instantly and the dynamic pressure will increase. The calculation for the maximum static inlet pressures is shown below.

Calculation:

Angular Velocity:

$$\omega = \frac{2\pi RPM}{60} \quad \left[\frac{rad}{s}\right] \tag{A.1}$$

Centrifugal Force:

$$F = m\frac{U^2}{r} \tag{A.2}$$

Since we are analyzing a fluid, it would be useful to put mass in terms of the fluid density, thus the equation becomes:

$$F = \rho\frac{U^2}{r}V \tag{A.3}$$

This is now rearranged in terms of forcer per unit volume (or pressure per unit length) as seen below:

$$\frac{F}{V} = \rho \frac{U^2}{r} \tag{A.4}$$

This can now be written in terms of pressure:

$$\int dP = \int \rho r \omega^2 dr \tag{A.5}$$

Thus:

$$\Delta P = \frac{\rho \omega^2 (r_2^2 - r_1^2)}{2} \tag{A.6}$$

Using this equation, a table is generated to show the pressure gradient from the impellors inner radius to the outer radius with pump speed varying from 100 to 3600 revolutions per minute.

Table A.1 Pressure Gradient at different pump speeds

RPM	***ω (rad/sec)***	***dP (lb/ft^2)***	***dP (lb/in^2)***	***dP (in w.c)***	***dP (N/m^2)***
100	10.47	12.23	0.08	2.35	59.73
200	20.94	48.93	0.34	9.41	238.90
300	31.42	110.10	0.76	21.18	537.53
400	41.89	195.72	1.36	37.66	955.61
500	52.36	305.82	2.12	58.84	1493.14
600	62.83	440.38	3.06	84.73	2150.13
700	73.30	599.41	4.16	115.32	2926.56
800	83.78	782.90	5.44	150.63	3822.45
900	94.25	990.86	6.88	190.64	4837.78
1000	104.72	1223.28	8.49	235.35	5972.57
1100	115.19	1480.17	10.28	284.78	7226.81
1200	125.66	1761.52	12.23	338.91	8600.50
1300	136.14	2067.34	14.36	397.75	10093.65
1400	146.61	2397.63	16.65	461.29	11706.24
1500	157.08	2752.38	19.11	529.55	13438.29
1600	167.55	3131.59	21.75	602.51	15289.78
1700	178.02	3535.28	24.55	680.17	17260.73
1800	188.50	3963.42	27.52	762.55	19351.13
1900	198.97	4416.04	30.67	849.63	21560.98
2000	209.44	4893.12	33.98	941.42	23890.29
2100	219.91	5394.66	37.46	1037.91	26339.04
2200	230.38	5920.67	41.12	1139.11	28907.25
2300	240.86	6471.15	44.94	1245.02	31594.91
2400	251.33	7046.09	48.93	1355.64	34402.01
2500	261.80	7645.49	53.09	1470.96	37328.57
2600	272.27	8269.37	57.43	1590.99	40374.59
2700	282.74	8917.70	61.93	1715.73	43540.05
2800	293.22	9590.51	66.60	1845.17	46824.96
2900	303.69	10287.78	71.44	1979.33	50229.33
3000	314.16	11009.51	76.45	2118.18	53753.15
3100	324.63	11755.71	81.64	2261.75	57396.42
3200	335.10	12526.38	86.99	2410.02	61159.14
3300	345.58	13321.51	92.51	2563.00	65041.31
3400	356.05	14141.11	98.20	2720.69	69042.93
3500	366.52	14985.17	104.06	2883.08	73164.01
3600	376.99	15853.70	110.10	3050.19	77404.53

Appendix B

TurboPiston Pump Bearing Load Calculation

In this section, bearing load calculations are performed to size the shaft bearings supporting the cylinder side of a 12" TurboPiston Pump.

Given:

Fluid:	Water
Cylinder Weight:	70 lbs
Piston Circle Radius "R_P":	4.34 in
Cylinder Diameter "D_c":	2.54 in
Distance "a":	5.44 in
Distance "b":	15.51 in
Cylinder Angle "θ_c":	18 degrees
Cylinder Pressure Expansion Cycle:	0 psia
Cylinder Pressure Compression Cycle:	310 psia
Discharge Pressure:	300 psia

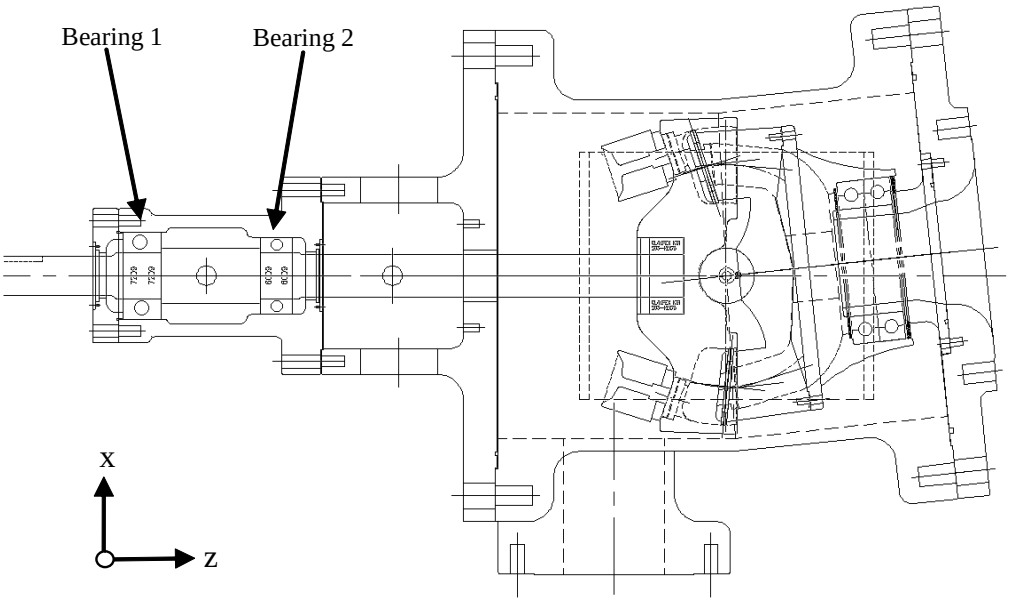

Figure B.1 TurboPiston Pump with bearings being analyzed.

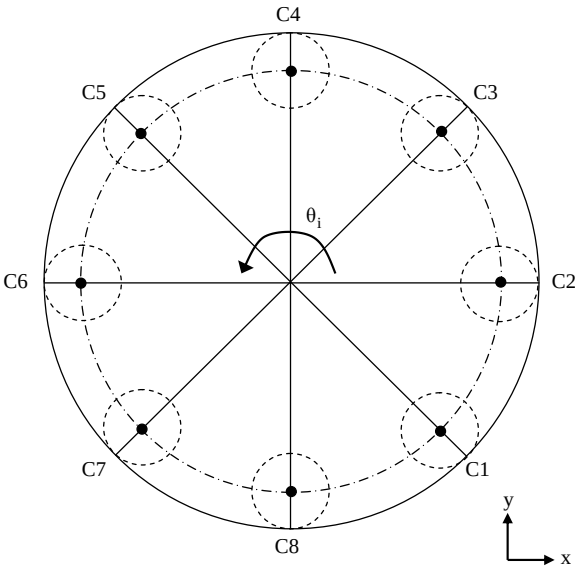

Figure B.2 Diagram showing cylinder position and labeling.

The pressure differential created between the inner cylinder wall and outer rotor wall creates a force on the rotor. This force is transferred through the shaft and must be supported by the bearings. Figure B.1 shows the orientation of each cylinder on the TurboPiston Pump, while Figure B.2 shows a side view of the pump. The force, designated F_P, created by the pressure differential is normal to the cylinder surface on which it acts and can be further be broken down into F_z and F_R for the z and radial direction respectively.

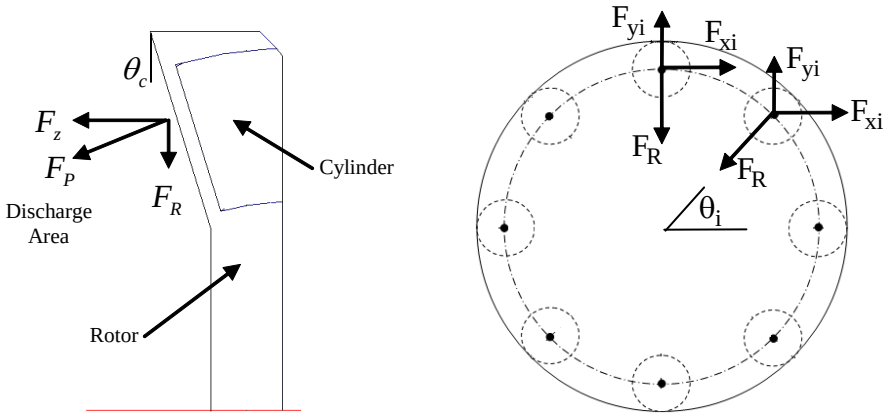

Figure B.3 Free body diagram of forces acting on the rotor due to a differential pressure across the cylinder

The equation used to calculate the force due to pressure can be seen below in Eq B.1.

$$F_P = \Delta P * A_c \tag{B.1}$$

Equation B.1 is further broken down into a z-component force and a radial-component force as shown in equation B.2 and B.3 respectively.

$$F_z = F_P COS(\theta_c) \tag{B.2}$$

$$F_R = F_P SIN(\theta_c) \tag{B.3}$$

The radial force isn't very useful for calculating the bearing load, thus it's convenient to further break it down into x and y components as seen in equation B.4 and B.5.

$$F_{xi} = -F_R COS(\theta_i) \tag{B.4}$$

$$F_{yi} = -F_R SIN(\theta_i) \tag{B.5}$$

Applying the input data to equations B.1 through B.5, Table B.1 is generated to show the force acting on the rotor due to each cylinder.

Table B.1 Forces acting on each cylinder of rotor

Cylinder\Force	Fp (lbs)	Fz (lbs)	Fr (lbs)	Fx (lbs)	Fy (lbs)
1	-515	-490	159	-112	112
2	-515	-490	159	-159	0
3	-515	-490	159	-112	-112
4	-515	-490	159	0	-159
5	51	49	16	11	-11
6	51	49	16	16	0
7	51	49	16	11	11
8	51	49	16	0	16

The force in the z direction puts a moment on the rotor and the bearings must counteract this load. The moments can be broken down into M_{xz} and M_{yz} as shown in equations B.6 and B.7 respectively.

$$M_{xz} = \sum_{i=1}^{8} -abs[F_{zi} R_P COS(\theta_i)] \tag{B.6}$$

$$\begin{aligned} M_{yz} = &\left(-abs[F_{zi} R_P SIN(\theta_i)]\right)_{i=1} + \sum_{i=2}^{4} abs[F_{zi} R_P SIN(\theta_i)] \\ &+ \left(-abs[F_{zi} R_P SIN(\theta_i)]\right)_{i=5} + \sum_{i=6}^{8} abs[F_{zi} R_P SIN(\theta_i)] \end{aligned} \tag{B.7}$$

Table B.2 is generated by summing the x, y, and z forces to get the total reaction in each given direction and by calculating the moments in each plane. Using this, a free body diagram is made as seen in Figure B.3 with the applied loads and bearing reactions.

Table B.2 Total Force and Moments acting of rotor

Total Force (lbs)		**Total Moment (in-lbs)**	
Fxt	-346	**Mxz**	-5642
Fyt	-213	**Myz**	2337
Fzt	-441		

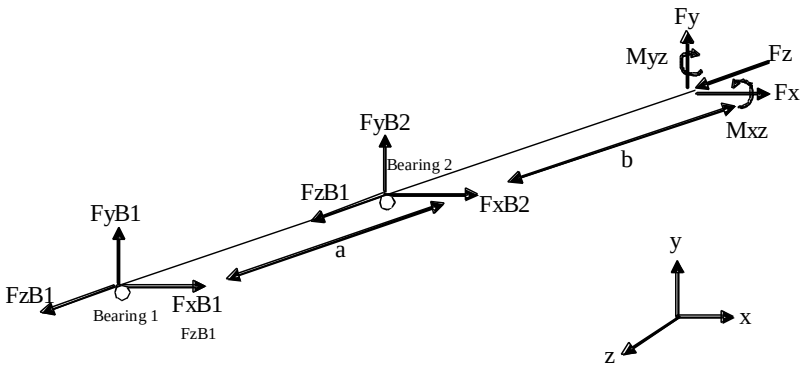

Figure B.4 Free body diagram of bearing-rotor assembly with all forces and moments acting on the system

Applying the general equations of static's to the free body diagram in Figure B.3, equations B.9 through B.13 are created and then solved for using methods such as a matrix for a system of linear equations. The results are tabulated in Table B.3.

$$\sum F_x : \; F_{B1x} + F_{B2x} + F_{xt} = 0 \tag{B.9}$$

$$\sum F_y : \; F_{B1y} + F_{B2y} + F_{yt} = 0 \tag{B.10}$$

$$\sum F_z : \; F_{B1z} + F_{B2z} + F_{zt} = 0 \tag{B.11}$$

$$\sum M_{xz} : \; F_{B1x}(a+b) + F_{B2x}(b) + M_{xz} = 0 \tag{B.12}$$

$$\sum M_{yz} : \; -F_{B1y}(a+b) - F_{B2y}(b) + M_{yz} = 0 \tag{B.13}$$

Table B.3: Resultant bearing loads

Bearing Load Results			
$\mathbf{F_{B1x}}$ (lbs)	50	$\mathbf{F_{B2x}}$ (lbs)	295
$\mathbf{F_{B1y}}$ (lbs)	-178	$\mathbf{F_{B2y}}$ (lbs)	390
$\mathbf{F_{B1}}$ (lbs)	184	$\mathbf{F_{B2}}$ (lbs)	489
$F_{B1z} + F_{B2z} = 441$(lbs)			

Vita

Jason Kent was born in New Orleans Louisiana in 1985. He started his college career at the University of New Orleans (UNO) in 2004 where he pursued a Bachelors of Science degree in Mechanical Engineering. As an undergraduate, Jason participated in many extracurricular actives such as American Society of Mechanical Engineering (ASME), Pi Tau Sigma (Mechanical Engineering Honors Society), and the University of New Orleans Baja Team. Upon the completion of his B.S. in Mechanical Engineering in 2008, he received a Research Assistantship at UNO and started his Masters of Science in Mechanical Engineering under Professor Dr. Ting Wang. He completed his M.S. in Mechanical Engineering in 2010. He then went on to start his professional career at Space Exploration Technologies (SpaceX) as a Propulsion Development Engineer.